

RESEARCH ARTICLE

Open Access



Global terrain classification using 280 m DEMs: segmentation, clustering, and reclassification

Junko Iwahashi^{1*}, Izumi Kamiya², Masashi Matsuoka³ and Dai Yamazaki⁴

Abstract

Polygon-based terrain classification data were created globally using 280 m digital elevation models (DEMs) interpolated from the multi-error-removed improved-terrain DEM (MERIT DEM). First, area segmentation was performed globally with the logarithmic value of slope gradient and the local convexity calculated from the DEM. Next, by adding surface texture, *k*-means clustering was performed globally and the polygons were grouped into 40 clusters. Then, we tried to reclassify these 40 clusters into geomorphologic terrain groups. In this study, we attempted reclassification and grouping using local information from Japan as a test case. The 40 clusters were compared with Japanese geological and geomorphological data and were then reclassified into 12 groups that had different geomorphological and geological characteristics. In addition, large shape landforms, mountains, and hills were subdivided by using the combined texture. Finally, 15 groups were created as terrain groups. Cross tabulations were performed with geological or lithological maps of California and Australia in order to investigate if the Japanese grouping of the clusters was also meaningful for other regions. The classification is improved from previous studies that used 1-km DEMs, especially for the representation of terrace shapes and landform elements smaller than 1 km. The results were generally suitable for distinguishing bedrock mountains, hills, large highland slopes, intermediate landforms (plateaus, terraces, large lowland slopes), and plains. On the other hand, the cross tabulations indicate that in the case of gentler landforms under different geologic provinces/climates, similar topographies may not always indicate similar formative mechanisms and lithology. This may be solved by locally replacing the legend; however, care is necessary for mixed areas where both depositional and erosional gentle plains exist. Moreover, the limit of the description of geometric signatures still appears in failure to detect narrow valley bottom plains, metropolitan areas, and slight rises in gentle plains. Therefore, both global and local perspectives regarding geologic province and climate are necessary for better grouping of the clusters, and additional parameters or higher resolution DEMs are necessary. Successful classification of terrain types of geomorphology may lead to a better understanding of terrain susceptibility to natural hazards and land development.

Keywords: Geomorphological map, Terrain classification, MERIT DEM, Japan, Geomorphometry, Landform

* Correspondence: iwahashi-j96pz@milit.go.jp

¹Geospatial Information Authority of Japan, Geography and Crustal Dynamics Research Center, Kitasato 1, Tsukuba, Ibaraki 305-0811, Japan
Full list of author information is available at the end of the article

Introduction

This study was performed to develop global terrain classification data that depict landform patterns as polygon data and that will help to estimate the ground characteristics of land. We use only digital elevation models (DEMs) as a data source and create a global polygon data set that can be flexibly classified. In common geomorphological maps, geomorphic provinces are shown as homogeneous regions of the same landform characteristics. Various landform characteristics are used: tectonic or volcanic landforms, exogenic landforms, and lithological features that are rather close to those used in engineering geological maps. Geomorphological maps are usually produced by interpretation of aerial photographs and various other documents that are concerned with slope materials and chronology. In the 1980s, some geomorphologists highlighted the numerical characteristics of landform elements (e.g., Evans 1980; Speight 1984; Pike 1988; Zevenbergen and Thorne 1987). Automated classification of topography by terrain measurements using DEMs (hereafter, terrain classification) has been developed by use of this technology. During the early period of terrain classification using DEMs, Dikau et al. (1991) presented unmanned landform classification maps. Research in the twenty-first century using only DEMs for terrain classification appears to be converging on two approaches; one is the classification of landform elements with reference to hydrological geomorphology and transportation of soils using high-resolution DEMs such as laser scanning data (e.g., van Asselen and Seijmonsbergen 2006; Drăguț and Blaschke 2006; MacMillan et al. 2003; del Val et al. 2015), and the other is classification of physiographic regions using medium or small-scale DEMs (e.g., Jasiewicz et al. 2014). In recent years, many studies have combined other parameters with DEMs; for example, Shafique et al. (2012) produced a seismic site characterization map by combining terrain classification with V_s30 (average shear wave velocity for the top 30 m); Guida et al. (2016) produced hydro-geomorphological scenario maps by combining API (air-photo interpretation) maps with flow accumulation data calculated from DEMs and hydro-chemographs from field surveys, and Martha et al. (2010) extracted landslides using terrain classification with satellite images. Hengl et al. (2017) produced global gridded soil information at 250-m resolution by machine learning using derivatives calculated from DEMs, land cover data from satellite data, lithologic units based on the Global Lithological Map (Hartmann and Moosdorf 2012), landform classes based on the USGS Map of Global Ecological Land Units (Sayre et al. 2014), and soil data from field surveys. Recent terrain classification

studies, especially with high-resolution DEMs, show that polygon-based outputs are increasingly using object-based area segmentation (Baatz and Schäpe 2000).

As Hough et al. (2010), Shafique et al. (2012), and Yong et al. (2012) described, one recent practical use of geomorphological information on the medium to small scale is the prediction of earthquake ground motion amplification. In Japan, the Cabinet Office recommends the local government to use geomorphological maps for earthquake disaster prevention measures. In addition, a nationwide 7.5 arc-second geomorphological map (Japan Engineering Geomorphologic Classification Map; JEGM, Wakamatsu and Matsuoka 2013) is used nationally for seismic hazard assessments. In California, Wills et al. (2000, 2015) proposed a V_s30 map with the same uses. The map was created by reclassification of the Geologic map of California (Jennings 1977) with the addition of soft-ground regions. As in the above studies, terrain classification is often cited as being related to the lithological condition of the ground.

The applications of terrain classification are diverse. Therefore, in this study, we prepare global terrain classification data as polygon data to which other thematic information could be added easily. In addition, we present the geomorphological grouping results of terrain in Japan as a test case and set out thematic information and conditions that need to be added in the future.

Iwahashi and Pike (2007) arranged a procedure for raster-GIS that became popular around 2000 and produced a 1-km grid worldwide raster terrain classification data set created from the Shuttle Radar Topography Mission 30 arc-second DEM (SRTM30) of the U.S. Geological Survey (USGS) using slope gradient, local convexity, and surface texture. At present, there are also some other global terrain classification data sets besides Iwahashi and Pike (2007) (Meybeck et al. 2001; Drăguț and Eisank 2012; Sayre et al. 2014). However, all data have coarse (1 km) resolution or do not represent terraces and fans that are important to human habitats. Iwahashi et al. (2015) tried to create polygon data of terrain classification by object-based area segmentation (Baatz and Schäpe 2000) using the geometric signatures of Iwahashi and Pike (2007). In the current study, we develop this approach and introduce a trial of a new procedure of polygon-based classification using 280 m DEMs interpolated from the multi-error-removed improved-terrain DEM (MERIT DEM; Yamazaki et al. 2017).

The important point of terrain classification using a DEM is that the result will depict geomorphologically appropriate classification if the DEM used is accurate. Iwahashi and Pike (2007), however, gave only numbers for map legends as a result of numerical classification. In this study, we try to attach geomorphological meanings to the classification results

according to cross tabulation with geological or geomorphological maps.

Methods

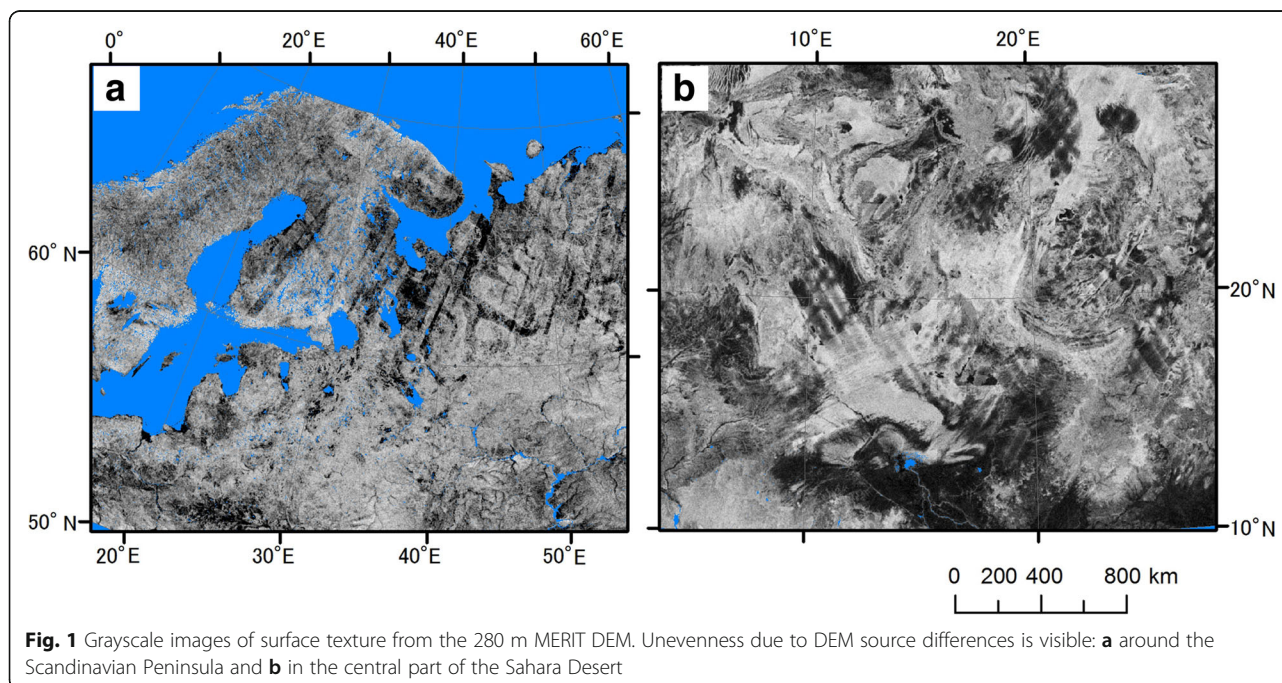
DEM

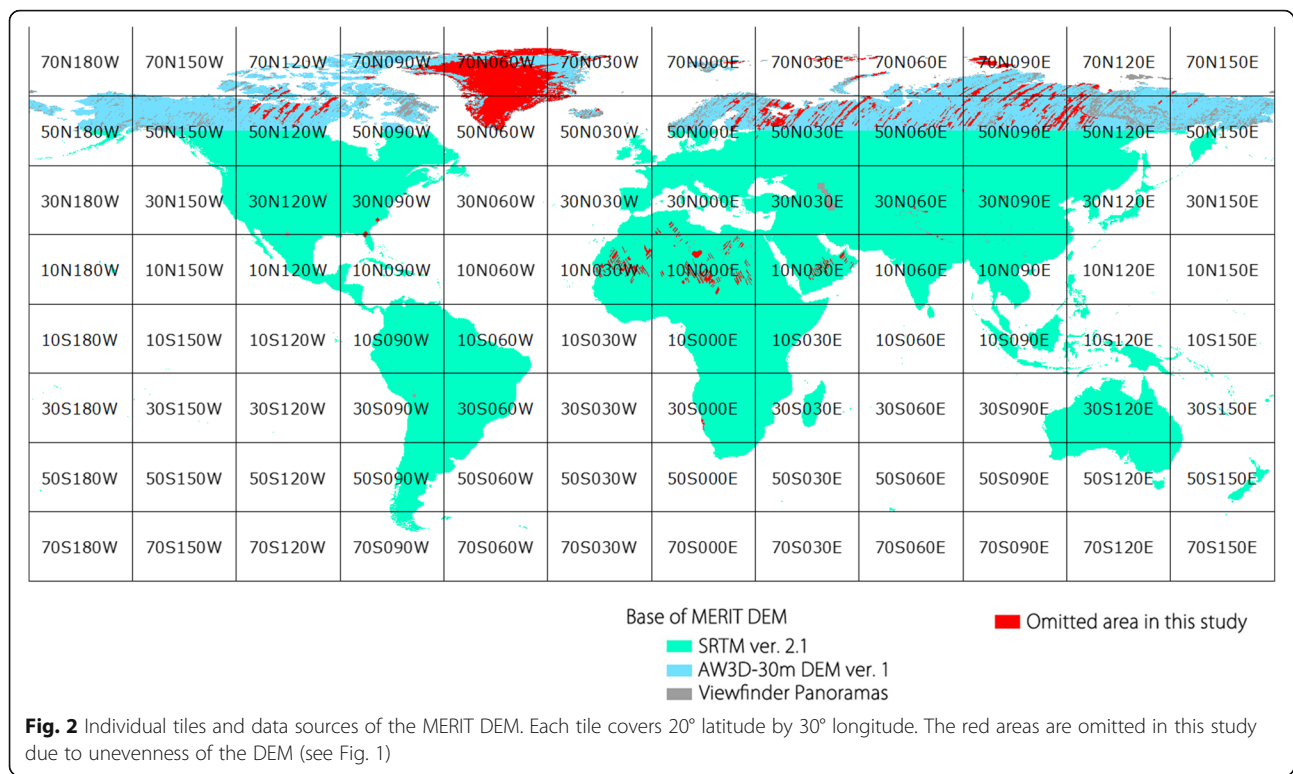
A serious problem in calculating geometric signatures from a fine-resolution DEM is caused by the precision unevenness in different DEM sources and also by the height errors in space-borne DEMs. The differences in spatial resolution or observation instrument (i.e., radar or optical) in source DEMs will cause different patterns of geometric signatures (De Reu et al. 2013; Maynard and Johnson 2014; Ariza-Villaverde et al. 2015). Such unevenness may not be apparent in an image of slope gradient, which is the destination of a primary difference (Evans 1980); however, the noise is more evident in an image uses a concept of secondary difference (e.g., Laplacian filter or curvature) in the calculation process (Guth 2006). Moreover, an image of surface texture (Iwahashi and Pike 2007), which uses a noise detector (median filter) in the calculation process, shows very clear unevenness (Fig. 1).

This study used the MERIT DEM that Yamazaki et al. (2017) produced by removing multiple error components from existing space-borne DEMs. The original MERIT DEM was developed with 3 arc second resolution by merging several baseline DEMs (Fig. 2). The data south of 60° N are based on the Shuttle Radar Topography Mission 3 arc-second DEM (SRTM3) ver. 2.1 (National Aeronautics and Space Administration; NASA), and the data north of 60° N are based on the

AW3D-30 m DEM ver. 1 (Japan Aerospace Exploration Agency; JAXA). Gaps in these DEMs are filled by the Viewfinder Panoramas DEM (available at <http://www.viewfinderpanoramas.org/dem3.html>). Yamazaki et al. (2017) used a 2D-Fourier-transform filter to remove striping and also used ICESat (Ice, Cloud, and land Elevation Satellite) laser altimetry data (NASA) to remove absolute bias and vegetation canopy bias. Speckle random noise was removed by applying an adaptive-scale smoothing filter (Gallant 2011). We resampled the MERIT DEM at 9 arc-second resolution by minimum elevation values for the terrain classification. The minimum values were chosen because the MERIT DEM includes buildings that need to be removed as far as possible to bring the values closer to ground data.

In Fig. 3a, the surface texture in another global DEM, GMTED2010 (Danielson and Gesch 2011) shows marked stripe noise (Nelson et al. 2009) originating from the SRTM DEM, whereas the MERIT DEM (Fig. 3b) is almost free from such unevenness. Small areas of the MERIT DEM, which still show unevenness (Fig. 1), were omitted from the terrain classification (Fig. 2). These errors coincided with the areas where high-quality DEMs (i.e., SRTM or AW3D) were not available as baseline data for the MERIT DEM. For example, the areas omitted north of 60° N correspond to the observation gap of the AW3D DEM, where the elevations originated from the Viewfinder Panoramas DEM, which has lower effective resolution than AW3D (Fig. 1a, darker areas). The areas omitted in desert regions also



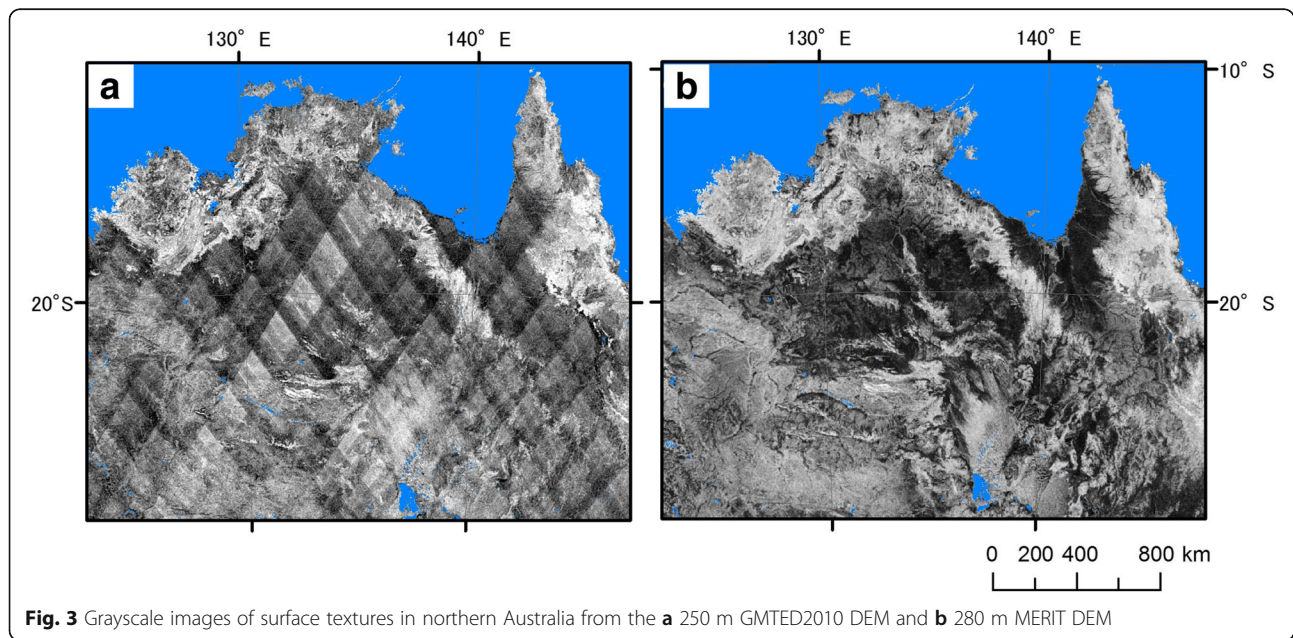


correspond to the observation gap of the AW3D DEM, where removal of the stripe noise was not satisfactory (Fig. 1b, brighter areas).

The MERIT DEM includes elevations of water bodies on land. Masking of water bodies was mostly achieved using the water bodies in the GlobCover2009 land cover map ver. 2.3 (Bontemps et al. 2013), whose resolution (10 arc-seconds) is close to 9 arc-seconds. The areas at

elevations under 0 m in the MERIT DEM were used as masks for two tiles (50S030 E and 30S150 W in Fig. 2) that show an obvious loss of islands in GlobCover2009.

The DEM resolution is set to 280 m as this corresponds to the spatial resolution of a 9 arc-second grid in the mid-latitudes. As Speight (1984) noted, at this resolution, a DEM draws landform patterns rather than landform elements.



Calculation of geometric signatures

Figure 4 shows the method for generating geometric signatures as classifying parameters and area segmentation using the MERIT DEM. First, the MERIT DEM was aggregated into 9 arc-seconds as described in the previous

section, a projection transform applied and 280 m DEMs were produced by interpolation with the nearest neighbor (DEM1) and the bilinear (DEM2) methods. These two types of DEMs were prepared in order to avoid the noise generated from features of raster image processing

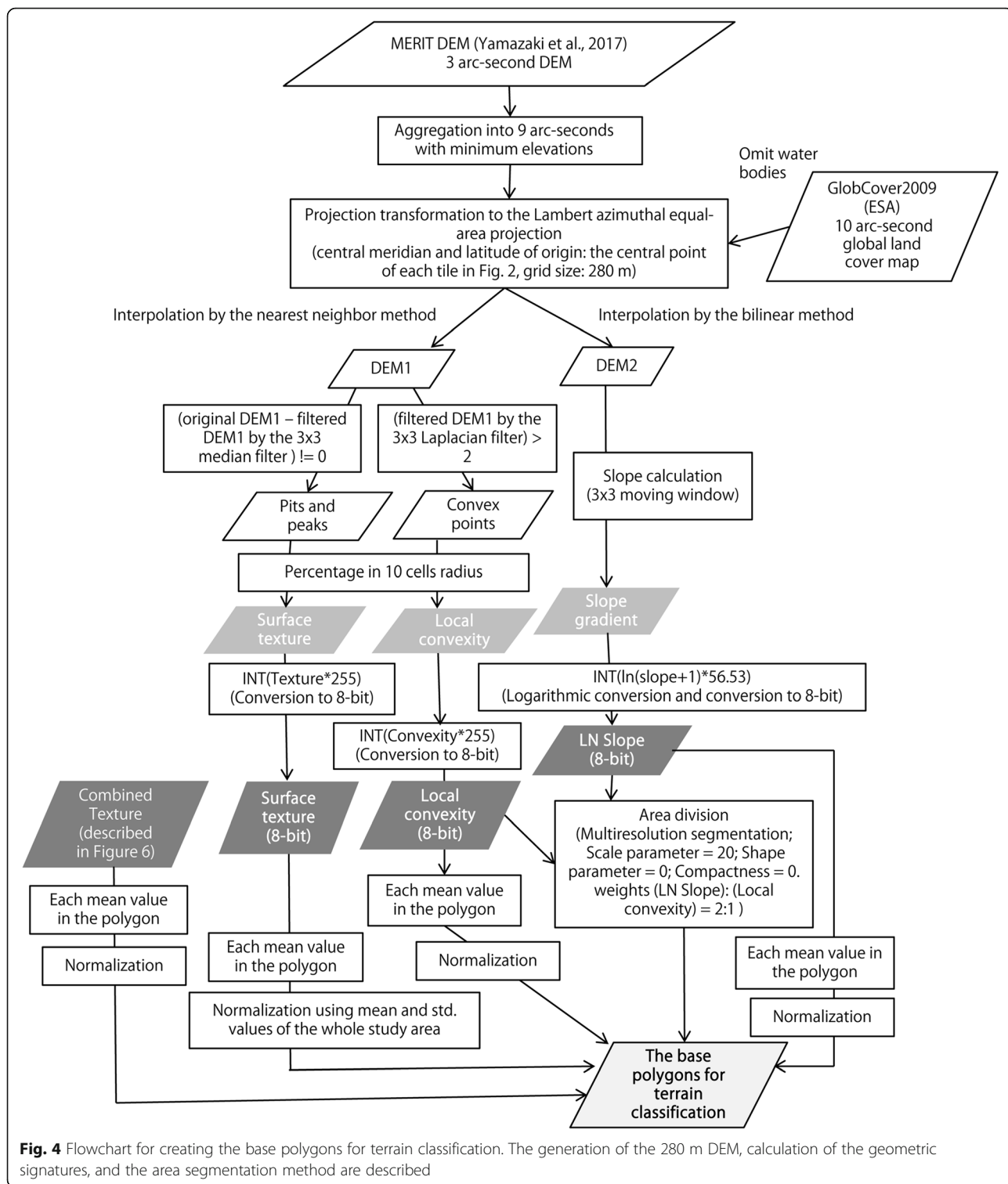


Fig. 4 Flowchart for creating the base polygons for terrain classification. The generation of the 280 m DEM, calculation of the geometric signatures, and the area segmentation method are described

in projection transformation becoming obvious in subsequent processing. Next, following Iwahashi and Pike (2007), three geometric signatures were calculated: slope gradient (in degrees calculated over 3×3 cells), local convexity (spatial density of convex points extracted by the Laplacian filter over 3×3 cells), and surface texture (spatial density of pits and peaks extracted by the median filter over 3×3 cells). The three geometric signatures can be calculated by common image processing software, e.g., ArcGIS Spatial Analyst (ESRI).

Iwahashi (1994) and Iwahashi and Kamiya (1995) introduced the slope gradient to extract mountain slopes from other slopes. In this study, slope gradient was converted logarithmically because, in Iwahashi and Pike (2007), thresholds of classification were defined to be graduated values by a nested-means method, that is, using successively averages of the total slope, the gentler half, the gentlest quarter, and the gentlest quarter-half. This follows a common geomorphological map style in which mountainous steep slopes tend to be lumped together while plains are divided into details. Thresholds of slope gradient for the nested-means method do not decrease linearly like those of surface texture and local convexity, but decrease logarithmically (Iwahashi and Pike 2007). As a consequence, logarithmic converted slope gradient (hereafter LN Slope) was used as a classifying parameter in order to replicate the decrease of thresholds in Iwahashi and Pike (2007).

The local convexity tends to be high in terrace surfaces (Iwahashi and Kamiya 1995). However, the local convexity calculated from different DEMs or using different thresholds that separate convex points and others showed very different patterns (Fig. 5, the Kanto District in Japan). The threshold value for extracting convex points used by Iwahashi and Pike (2007) was zero. In this study, we set the threshold value as 2. This value was chosen because we could obtain local convexity images to separate out terrace features and could reduce noise from artificial land as far as possible. Understanding of terrace features is important for information on human habitat, ground condition, and flooding in alluvial topography.

In Japan, surface texture shows relatively low values on debris slopes such as Holocene volcanic slopes and alluvial fans, or high permeability slopes such as weathered granites (Iwahashi and Kamiya 1995). Iwahashi and Pike (2007) showed that the surface texture calculated from the 1-km DEM using 3×3 cell windows depicted well the density of mountain ridges and valleys and divided large volcanic cones of Holocene mafic volcanos from older high-texture mountains. The surface texture values calculated from a 50-m DEM showed some correlation with $Vs30$ data

in Japan (Iwahashi et al. 2010). However, patterns of surface texture will change in response to the window size for extracting pits and peaks (Iwahashi and Pike 2007). However, small-scale geomorphological elements, such as cones of small volcanos could be distinguished in 3×3 surface texture of the 280 m DEM. A new signature, combined texture, was introduced to handle these scale issues. The combined texture was calculated as the minimum value of the normalized 3×3 and 13×13 surface texture values for each segmented polygon (Fig. 6). Finally, all geometric signatures were normalized to 8 bit to reduce data volume for dealing with processing ability.

Region segmentation

Homogeneous geomorphological elements (Fig. 4) were classified by area segmentation. We used a multi-resolution segmentation method (Baatz and Schäpe 2000) that was implemented in the software eCognition Developer ver.9 (Trimble Inc.). The multi-resolution segmentation method is a technique derived from moving image compression as used in the field of computer vision. The method aggregates neighboring cells that have values closer than a given threshold and then outputs polygons. The advantage is that the method can aggregate cells which include a little unevenness. Drăguț and Blaschke (2006) used this method for landform classification with 5-, 46-, and 57-m DEMs. Martha et al. (2010) used the method for landslide detection.

The shapes of polygons output by multi-resolution segmentation change with the choice of geometric signatures and their weights. Figure 7 shows some test cases in the Kanto District of Japan. When only LN Slope was used (Fig. 7b) for area segmentation, outlines of terraces and fans were described accurately. However, low terraces whose cliffs are not clearly defined such as the Omiya Upland (Fig. 7a) could not be outlined clearly. With high-accuracy domestic DEMs, a weight ratio of 1:1:1 for LN Slope:surface texture:local convexity gave good area segmentation (Iwahashi et al. 2015). However, with the 280 m DEM, the weight ratio 1:1:1 gave inaccurate terrace shapes (Fig. 7c). After trial and error, we chose a weight ratio of 2:0:1 for area segmentation using the 280 m DEM. The size of each destination polygon is mainly controlled by the scale parameter (Baatz and Schäpe 2000). We found that a scale parameter of 50 or 100 outputs segments that are too large and omits slightly elevated areas in lowlands (Fig. 7d, e). We finally chose a value of 20, which subdivided homogeneous landforms adequately but not excessively (Fig. 7f). The shape parameter, which provides a balance between shape and color for segmentation (Kavzoglu and Yildiz 2014), was set to zero following Drăguț and Eisank (2012). The compactness was also set to zero.

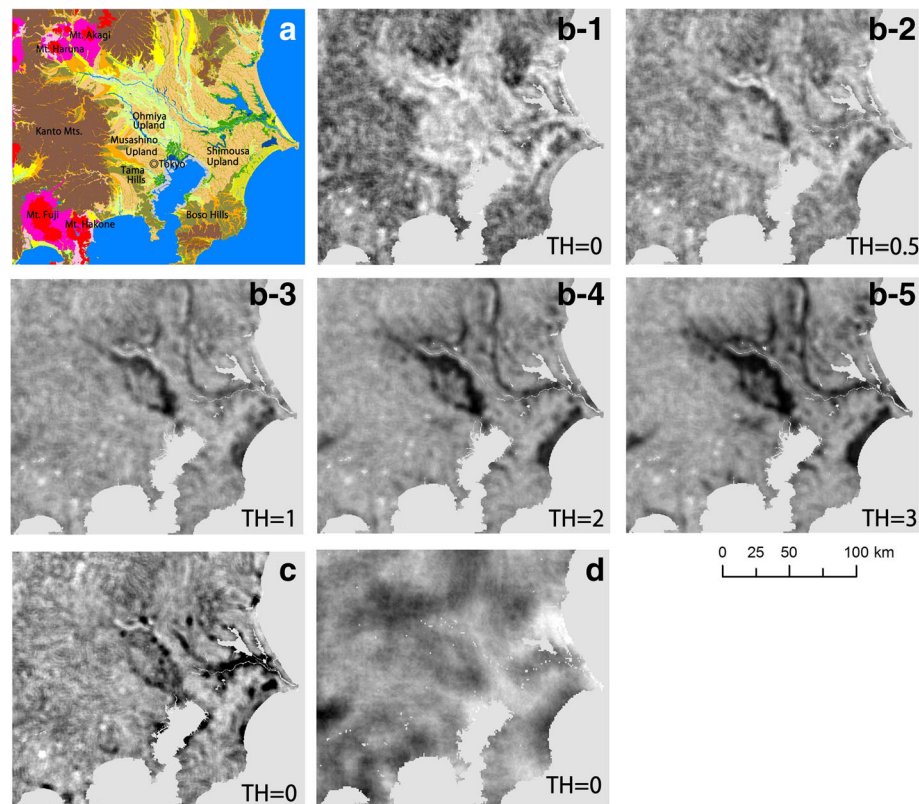


Fig. 5 Local convexity in the 280 m DEM from the Kanto District in Japan, calculated with different threshold values (TH) for separating out convex points. **a** JEGM (Wakamatsu and Matsuoka 2013) which shows terraces in orange. **(b-1 to b-5)** 280 m MERIT DEM. **c** 250 m GMTED2010 DEM. **d** 1 km SRTM30 DEM

Mean values for each geometric signature (LN slope, surface texture (3×3 and 13×13), combined texture, and local convexity) within the destination polygons were calculated and stored as representative values. We found much artificial unevenness in residential land. Therefore, we think that the standard deviation should not be used for representative values for the destination polygons, and we used only mean values. After all signatures were normalized and the combined textures were calculated from the normalized values of 3×3 and 13×13 surface texture, the base polygon datasets were prepared (Fig. 4).

Base classification

There are two kinds of classification method using geometric signatures: image thresholding and data mining. An image thresholding method using LN Slope is conceptually similar to the Iwahashi and Pike (2007) method, if thresholds are configured at equal intervals. The expected advantages are that large data sets can be classified using subdivided data, and classification from mixed DEMs of different data sources may be possible if corrected thresholds are used (Iwahashi et al. 2015). One weakness is that an

inappropriate configuration of thresholds will give nonsensical results. To attach geomorphological meanings to classification results, geometric signatures should be compared with reference materials, and thresholds should be configured after comparison (Iwahashi et al. 2015). However, reference materials are unlikely to be supported globally. Therefore, the image thresholding method is not suitable for global classification.

We instead adopted a machine learning method, *k*-means clustering (MacQueen 1967), for terrain classification (Fig. 8). The advantages of the clustering are that it can deal with large data and create groups without requiring training data. Unsupervised classification excluding subjective judgment will be suitable for comparing physical properties of ground with topography. We classified the base polygons created from the 280 m DEM using normalized LN slope, local convexity and surface texture by *k*-means clustering. The initial number of clusters was set to 40, assuming that the clusters would be reclassified into fewer groups. IBM SPSS Statistics ver.22 was used for *k*-means clustering and the calculation of all study areas (Fig. 2) converged to 40 clusters at the 682th iteration.

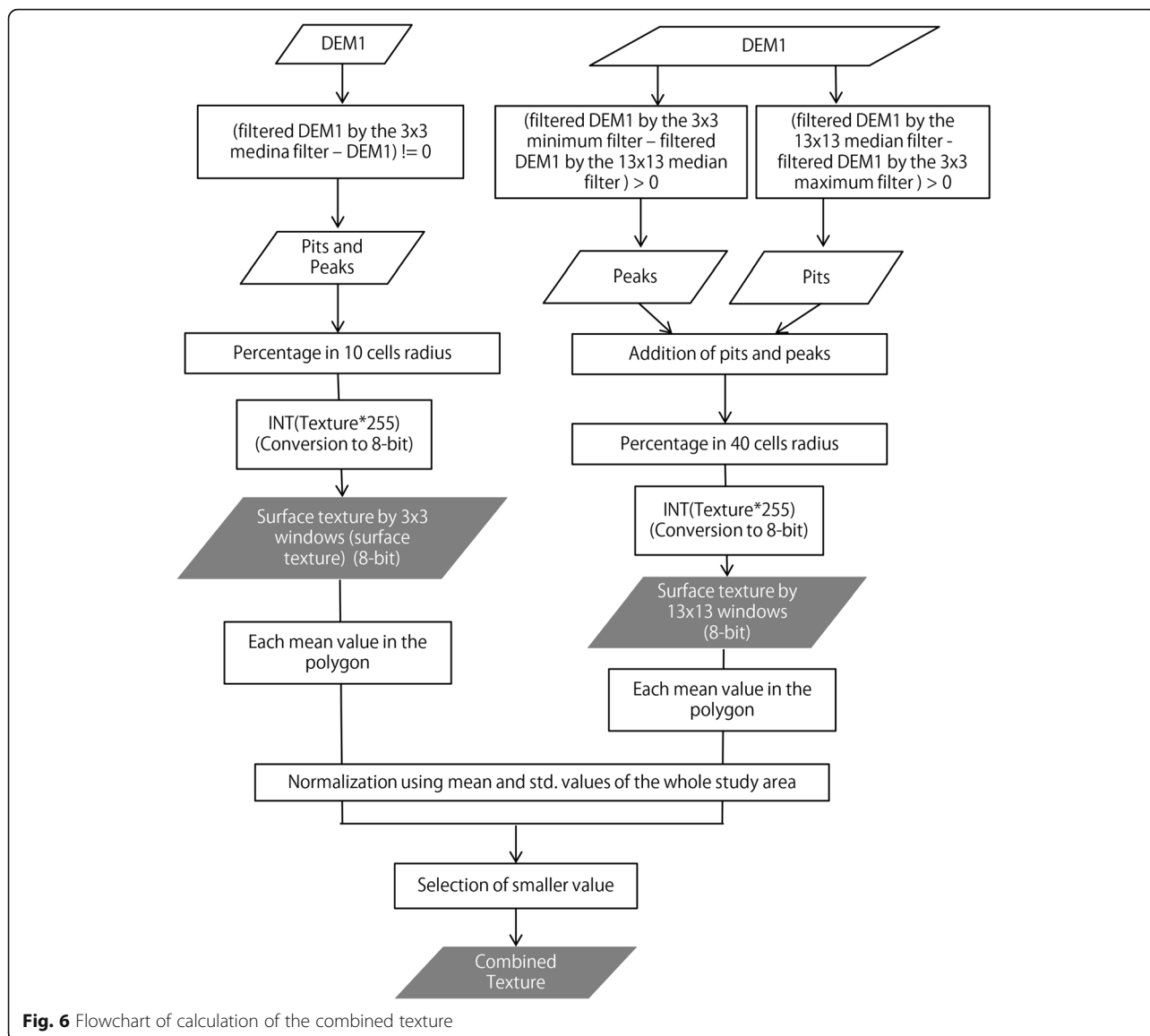


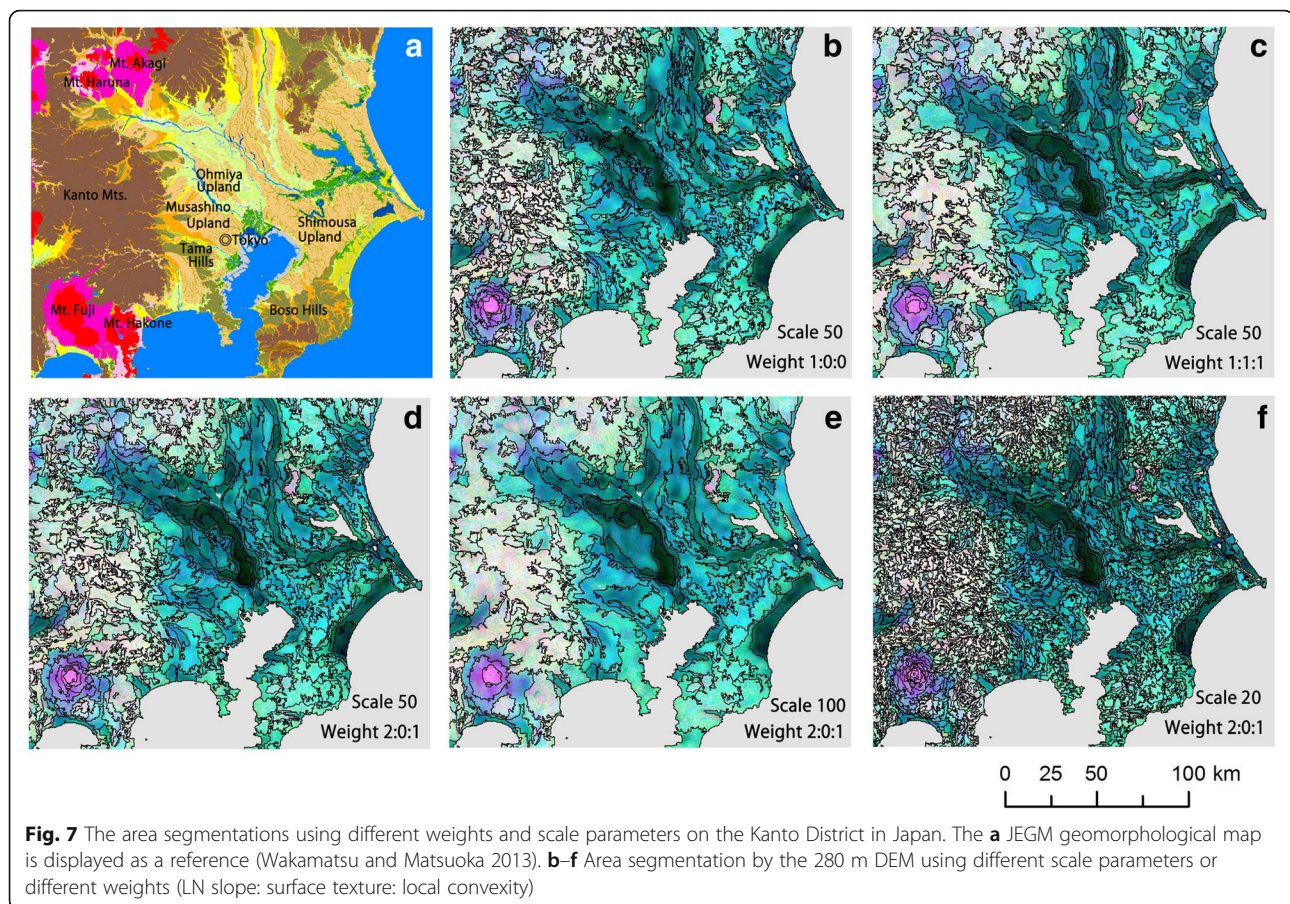
Fig. 6 Flowchart of calculation of the combined texture

Grouping of the clusters and reclassification

The 40 clusters indicate globally unified categories classified by machine learning. In order to identify the type of terrain they represent, we must compare them with existing thematic maps. Moreover, because 40 legends are too numerous for practical use, similar clusters must be merged. We thought that hierarchical clustering, using composition ratios and specialization coefficients of the comparison with thematic maps or data, was adequate to understand the similarity of the clusters. It is not necessary for thematic data to be global because it is possible to apply results in representative areas to other areas. Thematic data can be of any form as long as there is a correlation with terrain classification, and grouping of various themes is possible. On the other hand, comparing the clusters with thematic data that have no

relation to the topography may give meaningless groups. Therefore, we need thematic data that have a wide range, are related to topography, and a map scale that fits the 280 m resolution. Furthermore, as we explained for combined texture, due to the scale of the terrain, the optimal window size for calculating geometric signatures is likely to depend on the region, and additional reclassification may be necessary. In this study, we tested grouping and reclassification using Japanese GIS data in the form of geomorphological maps, geological maps, and landslide distribution maps. Flowcharts of the grouping and reclassification are shown in Fig. 8 and described in detail below.

In Japan, the distributions of the 40 clusters were numerically compared with existing nationwide geological, geomorphological, and landslide distribution maps (nos.



1 to 3 in Table 1). Cross tabulation results and graphs are shown in the Additional file 1 with the numbers of clusters.

For the cross tabulations, over 200 types of geologic units from the Seamless Digital Geological Map of Japan (SDGM) (Table 1) were reclassified for statistical convenience into 14 types according to lithology codes and rock age information in the data attributes. For example, “Sedimentary rocks” in the geological map was subdivided at the age 22 Ma (Middle Miocene), which is known as a boundary between linear and random plots in log–log plots of slope gradient and sedimentary rock age in Japan (Iwahashi et al. 2015). The Miocene is an important era for Japan, as it is the era when the Japan Sea began to open (Otofuji et al. 1985). Subdivision at the Miocene is also useful for imaging boundaries between consolidated and half- or unconsolidated sedimentary strata, because sedimentary rocks younger than the Neogene are often treated as soft rocks in the field of engineering geology in Japan (Japan Society of Civil Engineers 2016). We used full map units (22) of the JEGM (Table 1) for cross tabulation. The JEGM divides populated lowlands and terraces into several groups, but mountains are in one group, except for Holocene

volcanos. Older volcanos are depicted as mountains in the JEGM.

We performed hierarchical clustering using composition ratios and specialization coefficients from the comparison with geological and geomorphological maps and used percentages of landslide masses to assist grouping. The result shows three meaningful major branches (Fig. 9) compared with the characteristics of each cluster shown in the Additional file 1, i.e., (1) alluvial or coastal plains and non-volcanic terraces, (2) volcanos, hills, fans, and terraces, and (3) mountains. However, in the lower hierarchy, some groups seemed less useful. The result of hierarchical clustering (Fig. 9) was the first priority guide in grouping; however, visual observation of the thematic maps was used to recombine cases where the same mountain masses or terraces were found in different branches. In addition, we used point diagrams of convergence values of the clustering (Fig. 10) to check that the clusters within the same group did not differ markedly from each other.

The clusters were grouped into 12 groups. However, the grouping in mountains and hills tended to mix volcanic and non-volcanic mountains that could easily be distinguished by visual investigation with geological

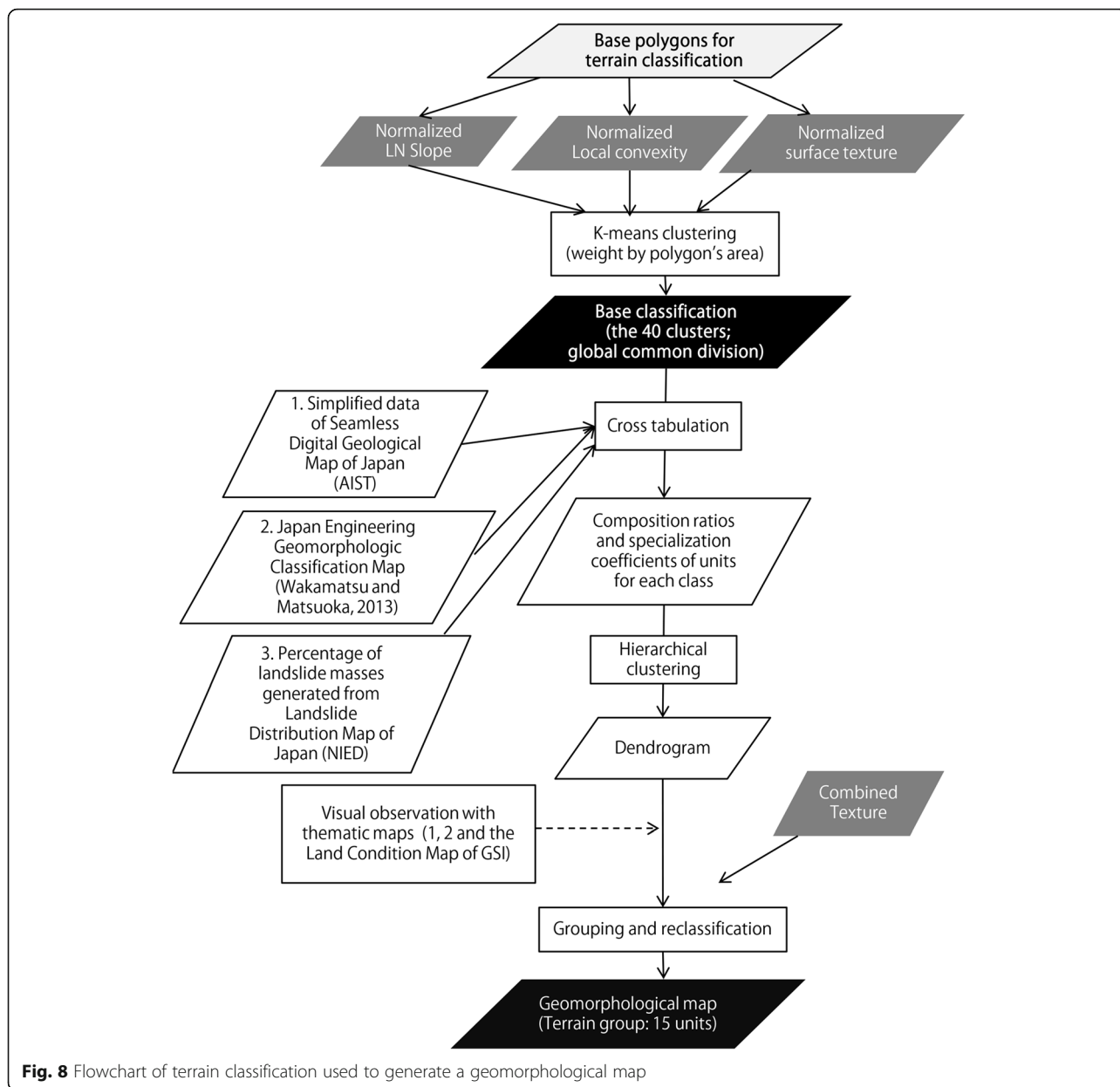


Fig. 8 Flowchart of terrain classification used to generate a geomorphological map

maps. Some, but not all, could be divided by surface texture calculated from a 1-km resolution DEM (Iwahashi and Pike 2007); therefore, the mixing was caused by the use of smaller sized windows for surface texture. We used the combined texture as an additional threshold parameter. Thresholds were decided by visual observation of the image of combined texture compared with the landform elements of JGEM and the 1:25,000 Land Condition Map of the Geospatial Information Authority of Japan (no. 4 in Table 1). The latter are geomorphological maps of urban plains and their surroundings, which have been published from the 1960s. The extra three groups found by this reclassification of mountains and hills gave a total of 15 definitive terrain groups. Table 2 gives quantitative descriptions of the 15 terrain groups.

Results

Cross tabulations with geological and geomorphological data

The terrain classification using DEM objectively distinguishes homogeneous slopes. In this study, we grouped slopes of similar properties by hierarchical clustering using Japanese thematic maps and reclassified mountains and hills by the combined texture. The final 15 groups were cross tabulated and visually compared with Japanese thematic maps again. Moreover, we also conducted the same analysis for overseas areas where public data can be obtained. We chose three scopes: an area that lies in a young orogenic belt like Japan (California), an area totally different from Japan in geological and climate settings

Table 1 Thematic map data used for comparison with the terrain classification of the current study

Range	Dataset (map)	Creator/publisher	Subject	Map scale/resolution	Usage in this study
1 Japan (nationwide)	Seamless Digital Geological Map of Japan (SDGM)	GSI ^a (ed.) (2015)	Geology	1:200,000	Grouping decision, subdivision of the groups
2 Japan (nationwide)	Japan Engineering Geomorphologic Classification Map (JEGM) ver.3	Wakamatsu and Matsuoka (2013)	Landform	250 m grid	Grouping decision, subdivision of the groups
3 Japan (nationwide)	Landslide Distribution Maps	NIED ^b	Landslides	1:50,000	Grouping decision
4 Japan (urban area)	Land Condition Map	GSI ^c	Landform	1:25,000	Subdivision of the groups
5 California	1/30 map	Wills et al. (2015)	Geological ground condition	1:24,000	Comparison
6 Australia	Geological Regions of Australia	Blake and Kilgour (1998), GA ^d (ed.)	Geology	1:5,000,000	Comparison
7 Australia	Regolith Map of Australia	Chan et al. 1986, GA (ed)	Major landform	1:5,000,000	Comparison

^aGeological Survey of Japan, AIST [2015]^bNational Research Institute for Earth Science and Disaster Resilience^cGeospatial Information Authority of Japan^dGeoscience Australia

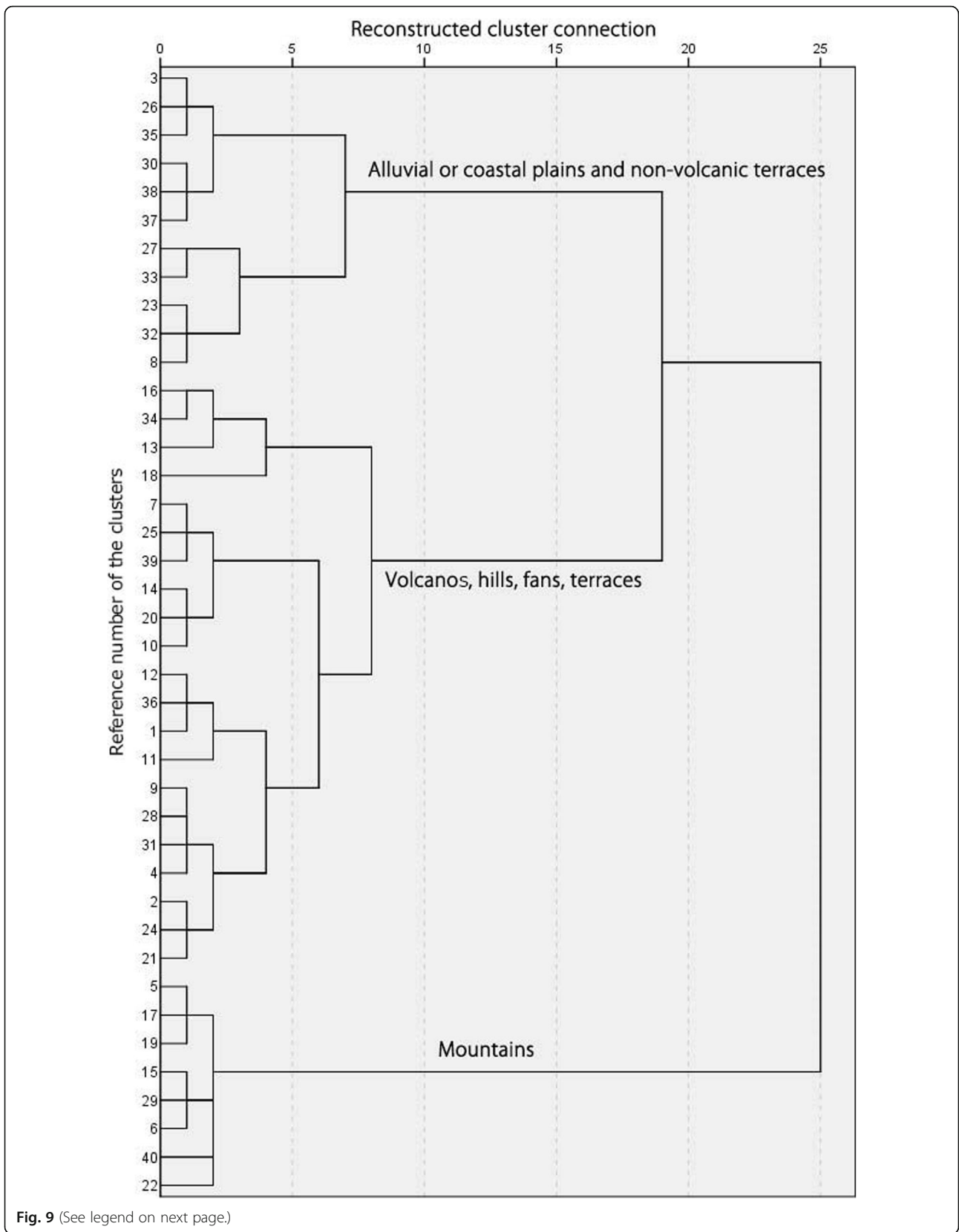


Fig. 9 (See legend on next page.)

(See figure on previous page.)

Fig. 9 Dendrogram of the 40 clusters obtained by hierarchical clustering in Japan. This figure shows a dendrogram calculated by the Ward method, using composition ratios and specialization coefficients of the comparison with JEGM and SDGM, and percentages of landslide masses (Table 1). Numbers in the left column of the graph are the reference numbers of the 40 clusters in the Additional file 1. The text in this graph shows typical landforms for the three branches

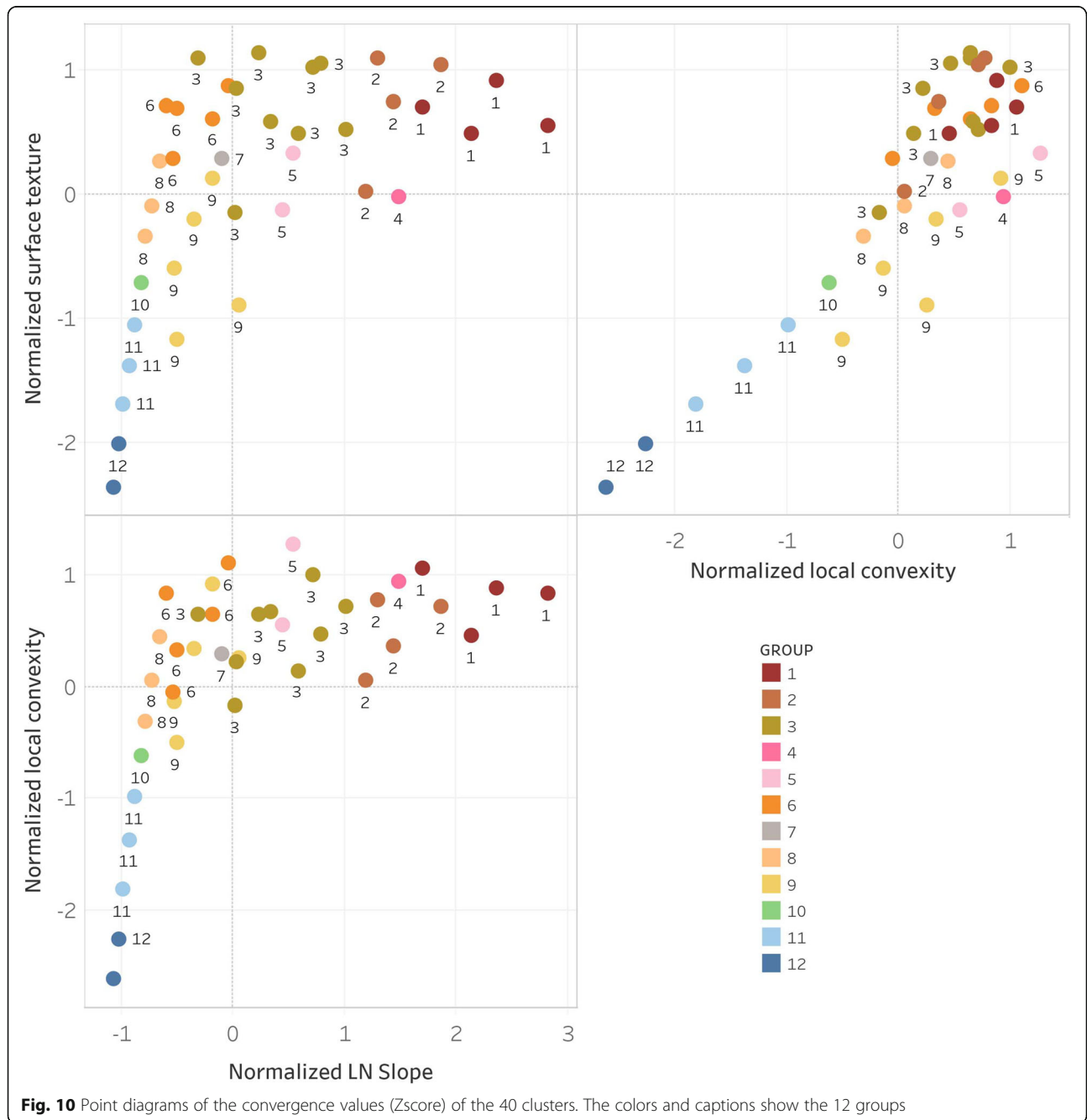


Fig. 10 Point diagrams of the convergence values (Zscore) of the 40 clusters. The colors and captions show the 12 groups

(Australia), and glacier regions that are rare in Japan but very important for landform formation in high-latitude areas. These analyses were important in order to construct the final legend.

Comparisons with the geological and geomorphological maps of Japan

We compared the statistics of the 15 groups and geomorphological and lithological data (Table 3). Table 3 lists not only composition ratios (*CR*) but also particularly large values (> two times) of specialization coefficients (*SC*) were described in Table 3, because map scales differ substantially (Table 1). *SC* describes the level of concentration of a certain map unit in the clusters. *SC* exceeding one indicates concentration of the distribution. This trend is more pronounced with larger *SC* values.

The result of grouping using Japanese geomorphological and geological data (SDGM and JEGM) generally implied the following. Groups 1 and 2 were bedrock mountains. In group 3, there were more sediments that were probably talus or dissected terraces, and the group indicated middle-relief mountains. Therefore, group 3 was hills. Among groups 1 to 3 (i.e., bedrock mountains and hills), there was a difference in major rock types in the sub-categories “a” and “b” as intended. Sub-category a seemed to be hard rocks, and b included debris and high-permeability rocks. On the other hand, Table 2 shows the difference between b of bedrock mountains and hills. Sub-category b in bedrock mountains was smooth on both large and small scales; however, b in hills was rough on the large scale. Groups 4 and 5 were highland slopes that

were steep but very smooth (Table 2), and they were closely related to Holocene mafic volcanos and their surroundings. Groups 6 to 12 were terraces, fans, and plains formed by unconsolidated strata. Their slope gradients were small and their average surface texture gradually decreased (Table 2). Groups 6 and 8 coincided closely with the Japanese major terrace type, i.e., terraces covered with volcanic ash soils (Wakamatsu and Matsuoka 2013). Group 7 was also terraces in a broad sense; however, specifically, it was rather fans or valley bottoms that were mainly distributed in shallow valleys in terraces. Group 9 mainly represented Japanese major alluvial fans that were formed by sands and gravels. Groups 10 to 12 covered alluvial plains, coastal plains, and their surroundings. Group 10 was plains at the foot of mountains. Groups 11 and 12, especially group 12, were very gentle slopes and widely distributed in muddy and silty plains.

The categories with low *CR* (<5%) that were not described in Table 3 were mainly as follows. Plutonic rocks (Middle Miocene to Holocene), ultramafic rocks, and felsic intrusive rocks had high *SC* values in group 1a. High *SC* values also appeared in groups 3b, 6, and 9 for Holocene tephra; groups 5, 6, and 7 for rocky strath terraces; groups 8, 10, and 11 for sand bars and dunes in coastal plains; and groups 6, 8, and 10 for filled land. Additional visual observation revealed that distinctive terrain with long slopes, such as caldera escarpments (e.g., Aso caldera, Kumamoto Prefecture, Kyushu), fault-block mountains (e.g., Yourou Mts., Gifu Prefecture, Honshu), and inselberg (e.g., Mt. Tsukuba, Ibaraki Prefecture, Honshu) were classified as group 1b.

Table 2 Quantitative values of the terrain groups, calculated globally

Terrain group	Cluster reference numbers (see Additional file 1 for Japanese conditions)	Average of slope gradient		Average of surface texture		Average of local convexity		Threshold of combined texture	Average of combined texture
		Degrees	Z score ^a	%	Z score	%	Z score		
1a	6, 15, 22, 40	14.8	2.25	70	0.77	43	0.85	> 0.41	0.72
1b		14.9	2.25	63	0.42	42	0.75	≤ 0.41	0.15
2a	5, 17, 19, 29	7.8	1.54	73	0.94	41	0.62	> 0.15	0.69
2b		6.5	1.34	68	0.65	38	0.43	≤ 0.15	−0.20
3a	4, 7, 10, 14, 20, 24, 25, 31, 39	2.8	0.50	71	0.79	40	0.55	> 0.1	0.51
3b		1.7	0.10	71	0.83	39	0.46	≤ 0.1	−0.43
4	18	7.5	1.49	55	−0.03	45	0.94		−0.08
5	16, 34	2.7	0.49	57	0.06	44	0.85		−0.03
6	2, 21, 28, 37, 38	0.8	−0.38	67	0.63	40	0.55		−0.06
7	9	1.3	−0.10	61	0.28	37	0.29		0.10
8	3, 26, 30	0.4	−0.72	55	−0.05	34	0.08		−0.46
9	1, 11, 12, 13, 36	0.9	−0.35	47	−0.46	35	0.18		−0.58
10	35	0.3	−0.82	42	−0.72	25	−0.62		−0.91
11	27, 32, 33	0.2	−0.93	30	−1.37	16	−1.38		−1.45
12	8, 23	0.1	−1.04	14	−2.20	3	−2.45		−2.20

^a1 Normalized value using global average and standard deviation

Table 3 CR^a and SC^b of geomorphological and geological units for each terrain group in Japan

Terrain group	Landform element of JEGM	Geological unit of SDGM
1a	Mountain (84%), volcano ^c (8%), others (8%)	Accretionary complex (30%), mafic volcanic rocks (Jurassic to Pleistocene) (20%), plutonic rocks (Silurian to Middle Miocene) (13%), felsic volcanic rocks (9%), metamorphic rocks (9%) (× 2.3), others (19%)
1b	Mountain (53%), volcano (32%)(× 7.0), volcanic footslope (9%), others (6%)	Mafic volcanic rocks (Jurassic to Pleistocene) (39%) (× 3.1), accretionary complex (13%), Plutonic rocks (Silurian to Middle Miocene) (10%), sediments (8%), felsic volcanic rocks (7%), pyroclastic flow deposits (6%)
2a	Mountain (79%), others (21%)	Accretionary complex (25%), mafic volcanic rocks (Jurassic to Pleistocene) (18%), plutonic rocks (Silurian to Middle Miocene) (13%), sediments (13%), felsic volcanic rocks (12%), sedimentary rocks (Silurian to Middle Miocene) (7%), metamorphic rocks (6%), others (6%)
2b	Mountain (70%), hill (9%), volcano (7%), others (14%)	Sediments (23%), accretionary complex (22%), mafic volcanic rocks (Jurassic to Pleistocene) (17%), sedimentary rocks (Silurian to Middle Miocene) (13%) (× 2.3), felsic volcanic rocks (9%), plutonic rocks (6%), others (10%)
3a	Mountain (36%), hill (23%), gravelly terrace (11%), valley bottom lowland (10%) (× 2.0), volcanic footslope (5%), others (15%)	Sediments (38%), accretionary complex (13%), Plutonic rocks (Silurian to Middle Miocene) (12%), mafic volcanic rocks (Jurassic to Pleistocene) (9%), pyroclastic flow deposits (8%), sedimentary rocks (Silurian to Middle Miocene) (7%), felsic volcanic rocks (7%), others (6%)
3b	Hill (32%) (× 3.1), mountain (20%), gravelly terrace (10%), volcanic footslope (9%), valley bottom lowland (8%), terrace covered with volcanic ash soil (6%), volcanic hill (6%) (× 2.4), others (9%)	Sediments (54%), pyroclastic flow deposits (13%) (× 2.3), accretionary complex (7%), sedimentary rocks (Silurian to Middle Miocene) (7%), mafic volcanic rocks (Jurassic to Pleistocene) (5%), others (14%)
4	Volcano (55%) (× 12.5), volcanic footslope (36%) (× 7.7), others (9%)	Mafic volcanic rocks (Holocene) (47%) (× 84.3), volcanic debris (Miocene to Holocene) (21%) (× 12.6), mafic volcanic rocks (Jurassic to Pleistocene) (16%), pyroclastic flow deposits (8%), others (8%)
5	Volcanic footslope (60%) (× 12.8), gravelly terrace (10%), terrace covered with volcanic ash soil (9%) (× 2.3), volcano (6%), others (15%)	Sediments (35%), volcanic debris (Miocene to Holocene) (23%) (× 13.9), pyroclastic flow deposits (18%) (× 3.1), mafic volcanic rocks (Holocene) (14%) (× 25.8), mafic volcanic rocks (Jurassic to Pleistocene) (7%), others (3%)
6	Terrace covered with volcanic ash soil (19%) (× 4.8), gravelly terrace (16%) (× 2.4), valley bottom lowland (14%) (× 3.0), hill (12%), volcanic footslope (7%), back marsh (7%) (× 2.5), alluvial fan (7%) (× 2.3), delta and coastal lowland (5%) (× 3.1), others (13%)	Sediments (79%) (× 2.3), pyroclastic flow deposits (8%), others (13%)
7	Gravelly terrace (29%) (× 4.2), terrace covered with volcanic ash soil (14%) (× 3.5), hill (13%), alluvial fan (12%) (× 4.3), valley bottom lowland (10%) (× 2.2), volcanic footslope (8%), others (14%)	Sediments (81%) (× 2.4), pyroclastic flow deposits (5%), others (14%)
8	Terrace covered with volcanic ash soil (19%) (× 4.8), alluvial fan (16%) (× 5.7), gravelly terrace (15%) (× 2.2), back marsh (14%) (× 5.2), delta and coastal lowland (8%) (× 4.7), others (28%)	Sediments (95%) (× 2.8), others (5%)
9	Alluvial fan (30%) (× 10.5), gravelly terrace (30%) (× 4.4), terrace covered with volcanic ash soil (16%) (× 4.1), volcanic footslope (10%) (× 2.1), others (14%)	Sediments (86%) (× 2.5), pyroclastic flow deposits (5%), others (9%)
10	Back marsh (28%) (× 9.9), alluvial fan (22%) (× 7.5), delta and coastal lowland (14%) (× 8.3), gravelly terrace (8%), natural levee (7%) (× 11.2), others (21%)	Sediments (99%) (× 2.9), others (1%)
11	Back marsh (36%) (× 13.1), delta and coastal lowland (18%) (× 10.9), alluvial fan (12%) (× 4.3), natural levee (11%) (× 17.1), reclaimed land (6%) (× 13.3), others (17%)	Sediments (100%) (× 2.9)
12	Back marsh (56%) (× 20.0), delta and coastal lowland (21%) (× 13.0), natural levee (14%) (× 21.0), reclaimed land (7%) (× 14.7), others (2%)	Sediments (100%) (× 2.9)

Legends with CR of 5% or more are shown. Clusters with SC over × 2.0 are shown in bold text and the factors are in parentheses

^aComposition ratio

^bspecialization coefficient

^climited to Holocene volcano in JEGM

Comparisons with geohazard data and densely inhabited district data in Japan

In Japan, the Ministry of Land, Infrastructure and Transport (MLIT) has published some national statistics as GIS data, “National Land Numerical Information”. Wakamatsu (2011) collected spatial data of historic (745 A.D. to 2008 A.D.) liquefaction in Japan. We analyzed the relationship between the subjects concerning such land conditions and each terrain group. Table 4 shows *CR* and *SC* of terrain group vs. densely inhabited districts (DID), sediment disaster hazard areas, and historic liquefaction. The sediment disaster hazard areas, which describe dangerous zones susceptible to collapse, mud or debris flows, and landslides, are not specified in regions with no or few downstream habitations. Therefore, we calculated corrected specialization coefficients (*CSC*) in Table 4 by using distribution percentages of the DID areas (*CSC*: SC/CR in the DID areas for each group).

The GIS data of historic liquefactions (Wakamatsu 2011) describe newer liquefactions after the World War II that can be delineated on maps or aerial photographs as polygons and describe the first liquefaction that appears in Japanese historical documents (745 A.D.) to the last liquefaction within the data collection period (2008 A.D.) as point data of the centers of liquefied areas. The point data include 3717 liquefaction sites, but many of these are near seashores and overlap with the water body

of the GlobCover 2009. Therefore, 2914 of the point data were used in the analysis.

The DID areas in Japan were remarkably concentrated in groups 6 to 12. Although the highest *SC* value was in group 8 that was mainly low terraces, the distributions of errors caused by reclaimed land around coastal areas may have raised *SC*. The liquefaction sites in polygon form were mainly distributed in groups 11 and 12, which were very gentle slopes. However, point data of liquefaction sites were concentrated on steeper slopes which correspond to terrains, alluvial fans, and hills. According to individual investigation of those sites, hilly cases were divided into three types: banking on residential areas, exceedingly strong earthquakes which occurred in hills of sedimentary rocks (e.g., the Chuetsu Earthquake on 23 October 2004), and insufficient DEM resolution that missed narrow plains along valleys or coastlines.

The zones susceptible to collapse in Japan and officially considered dangerous are defined by the MLIT as steep slopes (over 30° and 5 m high) and their surrounding habitats. These zones were concentrated not only in the groups representative of bedrock mountains (groups 1 and 2) but also in highland slopes that were thought to be formed by debris or high permeability rocks (groups 4 and 5), especially in group 4. *CSC* values were also very high in the case of the officially defined zones of landslides and debris flow.

Table 4 *CR*^a, *SC*^b, and *CSC*^c of DID^d and geohazards for each terrain group in Japan

Terrain group	All Japan	DID		Dangerous zones for the sediment disaster hazard area						Historic liquefaction			
		<i>CR</i> (%)	<i>SC</i> (%)	Collapse		Landslide		Debris flow		Center point (745 A.D. to 2008 A.D.)		Polygon (after WW2)	
	<i>CR</i> (%)	<i>CR</i> (%)	<i>SC</i>	<i>CR</i> (%)	<i>CSC</i>	<i>CR</i> (%)	<i>CSC</i>	<i>CR</i> (%)	<i>CSC</i>	<i>CR</i> (%)	<i>SC</i>	<i>CR</i> (%)	<i>SC</i>
1a	13.2	0.1	0.0	5.3	5.7	11.0	11.9	3.9	4.3	0.0	0.0	0.0	0.0
1b	2.6	0.1	0.0	1.0	7.3	2.1	16.0	1.5	11.0	0.0	0.0	0.0	0.0
2a	31.9	1.0	0.0	32.4	1.0	43.5	1.3	33.3	1.0	0.1	0.0	0.1	0.0
2b	4.0	0.5	0.1	3.4	1.9	7.7	4.2	4.5	2.5	0.0	0.0	0.0	0.0
3a	20.6	8.2	0.4	37.9	0.2	24.6	0.1	40.1	0.2	4.1	0.2	1.1	0.1
3b	9.6	7.7	0.8	12.9	0.2	10.0	0.1	9.7	0.1	9.2	1.0	4.0	0.4
4	0.3	0.0	0.0	0.1	44.0	0.1	60.8	1.0	402.9	0.0	0.0	0.0	0.0
5	0.6	0.5	0.8	0.5	1.7	0.2	0.6	2.5	8.5	0.0	0.1	0.0	0.0
6	6.5	23.0	3.5	4.7	0.0	0.6	0.0	1.7	0.0	17.6	2.7	9.0	1.4
7	1.2	3.9	3.3	0.9	0.2	0.2	0.0	1.4	0.3	1.3	1.1	0.4	0.3
8	4.6	34.3	7.5	0.6	0.0	0.1	0.0	0.2	0.0	34.4	7.5	29.9	6.6
9	1.1	3.1	2.9	0.2	0.1	0.1	0.0	0.2	0.1	0.2	0.2	0.7	0.6
10	1.4	6.3	4.6	0.1	0.0	0.0	0.0	0.0	0.0	29.0	21.1	12.8	9.3
11	2.2	9.5	4.3	0.0	0.0	0.0	0.0	0.0	0.0	3.7	1.7	34.9	15.8
12	0.4	1.9	5.1	0.0	0.0	0.0	0.0	0.0	0.0	0.3	0.7	7.2	19.0

^aComposition ratio

^bspecialization coefficient

^cspecialization coefficient corrected by the composition ratio of units in the DID area of terrain groups

^dDensely inhabited districts

In these cases, smooth steep slopes (groups 1b, 2b, and 4) show higher CSC values.

Comparison with the Vs30 data in Japan

The ground Vs30, which is observed or estimated by borehole data, is a predictor of earthquake ground motion amplification. We compared the calculated Vs30 based on published shear-wave velocity profile data in Japan (Strong-motion Seismograph Networks, K-NET and KIK-net by NIED; <http://www.kyoshin.bosai.go.jp>) with the terrain classification (Fig. 11). In extremely steep slope areas (Additional file 1) like groups 1a and 1b, there is a possibility that Vs30 values were measured on narrow valley floors that are not described by the 280 m DEM.

The box plot in Fig. 11 shows relatively low medians for smooth slopes (1b, 2b, and 3b) in mountains and

hills. However, among intermediate landforms, thought to be formed by half- or unconsolidated strata, fan-predominant slopes (groups 7 and 9) showed higher Vs30 values than terrace-predominant slopes (groups 6 and 8) that were usually rougher than fans. In plains, (groups 10 to 12), Vs30 values decreased along with slope gradients.

Comparisons with data from California, Australia, and glacier regions

Cross tabulations were performed with geological or lithological maps of California and Australia in order to investigate if the Japanese grouping of the clusters was also meaningful for other regions (Table 5). California lies on a young orogenic belt like Japan, but there are no Holocene volcanos and the climate is drier than in Japan. Australia mostly lies on very dried shields and

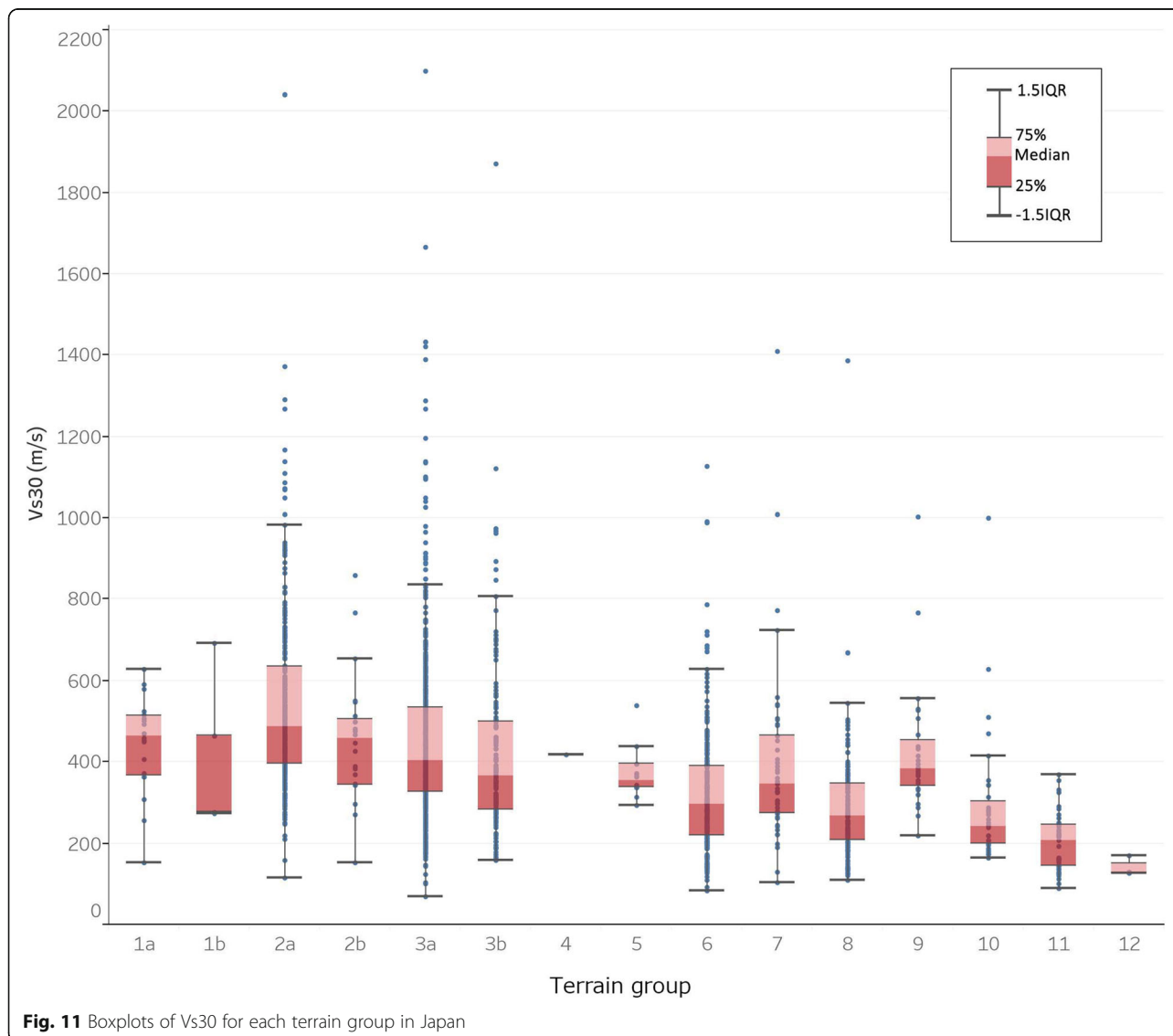


Fig. 11 Boxplots of Vs30 for each terrain group in Japan

Table 5 CR^a and SC^b of geomorphological and geological units for each terrain group in California and Australia

Terrain group	California, lithological unit of Wills et al. (2015)	Australia, geological unit reclassified ^c from Blake and Kilgour (1998)	Australia, major landform unit of Chan et al. (1986)
1a	Crystalline rocks (61%) (x2.1), Franciscan complex rocks (17%) (x2.7), Tertiary volcanic units (8%), Tertiary sandstone units (6%), others (8%)	Sedimentary rocks (51%), granites (19%), felsic volcanics (8%) (x5.8), mafic intrusives (6%) (x9.1), Cenozoic mafic volcanics (6%) (x4.1), metamorphics (6%), others (4%)	Mountains (59%) (x10.1), plateau (15%), hills (12%), low hills (7%)
1b	Crystalline rocks (59%) (x2.0), Tertiary volcanic units (19%), Tertiary sandstone units (5%), others (17%)	Sedimentary rocks (49%), granites (29%) (x2.9), metamorphics (5%), others (17%)	Hills (35%) (x3.2), mountains (34%) (x5.8), low hills (7%)
2a	Crystalline rocks (45%), Tertiary sandstone units (14%), Franciscan complex rocks (13%) (x2.0), Tertiary volcanic units (9%), Tertiary shale and siltstone units (7%), others (12%)	Sedimentary rocks (58%), granites (16%), felsic volcanics (6%) (x4.4), Cenozoic mafic volcanics (6%) (x4.1), others (14%)	Mountains (45%) (x7.7), hills (21%), low hills (11%)
2b	Crystalline rocks (36%), Tertiary volcanic units (15%), Tertiary sandstone units (14%), Holocene alluvium (steep slopes) (12%), Cretaceous sandstone (6%) (x2.8), Tertiary shale and siltstone units (6%), others (11%)	Sedimentary rocks (66%), granites (12%), metamorphics (7%), others (15%)	Hills (24%) (x2.2), mountains (23%) (x4.0), plateau (17%), low hills (12%), rises (7%)
3a	Crystalline rocks (32%), Tertiary volcanic units (18%), Tertiary sandstone units (11%), Holocene alluvium (steep slopes) (9%), Franciscan complex units (7%), Tertiary shale and siltstone units (6%), Pleistocene alluvium (6%), Pleistocene - Pliocene alluvial deposits (5%), others (6%)	Sedimentary rocks (55%), granites (17%), mafic volcanics (6%) (x2.2), felsic volcanics (6%) (x4.2), others (16%)	Hills (30%), low hills (23%) (x2.1), mountains (22%) (x3.9), plateau (13%)
3b	Holocene alluvium (steep slopes) (22%) (x2.1), crystalline rocks (16%), Tertiary volcanic units (14%), Tertiary sandstone units (14%), Pleistocene alluvium (12%), Pleistocene-Pliocene alluvial deposits (7%) (x2.9), Tertiary shale and siltstone units (7%), others (8%)	Sedimentary rocks (62%), Cenozoic regolith (10%), granites (10%), metamorphics (6%), others (12%)	Hills (23%) (x2.1), low hills (20%), mountains (14%) (x2.4), plateau (13%), rises (9%), erosional plain (6%)
4	Tertiary volcanic units (39%) (x3.5), crystalline rocks (25%), Holocene alluvium (steep slopes) (18%), Pleistocene alluvium (8%), others (10%)	Sedimentary rocks (58%), mafic volcanics (13%) (x4.8), Cenozoic mafic volcanics (8%) (x5.2), metamorphics (6%), Cenozoic regolith (5%), others (10%)	Hills (37%) (x3.4), low hills (22%) (x2.0), mountains (20%) (x3.5), lava plain (7%) (x10.3), plateau (6%)
5	Holocene alluvium (steep slopes) (44%) (x4.3), Pleistocene alluvium (19%), crystalline rocks (15%), Tertiary volcanic units (13%), others (9%)	Sedimentary rocks (65%), Cenozoic regolith (15%), Cenozoic mafic volcanics (7%) (x5.0), others (13%)	Low hills (30%) (x2.8), hills (22%) (x2.1), coastal dunes (7%) (x14.8), dunefield (7%), lava plain (6%) (x9.3), mountains (6%)
6	Tertiary sandstone units (19%) (x2.3), Tertiary volcanic units (19%), Pleistocene alluvium (18%), Holocene alluvium (steep slopes) (13%), crystalline rocks (10%), Holocene alluvium (moderate slopes) (8%), Pleistocene-Pliocene alluvial deposits (7%) (x3.0), others (6%)	Sedimentary rocks (47%), Cenozoic regolith (20%), granites (13%), metamorphics (6%), mafic volcanics (6%) (x2.1), others (8%)	Hills (25%) (x2.3), low hills (18%), mountains (11%), plateau (10%), rises (9%), dunefield (8%), sand plain (6%), erosional plain (5%)
7	Tertiary volcanic units (24%) (x2.1), Pleistocene alluvium (21%) (x2.0), Holocene alluvium (steep slopes) (21%) (x2.0), crystalline rocks (10%), Tertiary sandstone units (8%), Pleistocene - Pliocene alluvial deposits (5%), others (11%)	Sedimentary rocks (57%), Cenozoic regolith (15%), granites (11%), metamorphics (6%), others (11%)	Hills (23%) (x2.1), low hills (17%), plateau (14%), dunefield (12%), rises (10%), mountains (9%), erosional plain (6%)
8	Holocene alluvium (moderate slopes) (28%) (x4.2), Pleistocene alluvium (23%) (x2.2), tertiary volcanic units (21%), Holocene alluvium (very low slopes) (8%), tertiary sandstone units (8%), Holocene alluvium (steep slopes) (6%), others (6%)	Cenozoic regolith (42%), sedimentary rocks (36%), granites (8%), metamorphics (5%), others (9%)	Dunefield (23%) (x2.2), sand plain (13%), plateau (12%), erosional plain (11%), rises (9%), low hills (8%), hills (8%), depositional plain (6%)
9	Holocene alluvium (moderate slopes) (34%) (x5.1), Holocene alluvium (steep slopes) (32%) (x3.1), Pleistocene alluvium (21%) (x2.0), Tertiary volcanic units (5%), others (8%)	Sedimentary rocks (36%), Cenozoic regolith (32%), granites (18%), metamorphics (6%), others (8%)	Plateau (23%) (x2.1), erosional plain (16%), dunefield (14%), sand plain (10%), low hills (9%), rises (8%), hills (6%), depositional plain (6%)

Table 5 CR^a and SC^b of geomorphological and geological units for each terrain group in California and Australia (Continued)

Terrain group	California, lithological unit of Wills et al. (2015)	Australia, geological unit reclassified ^c from Blake and Kilgour (1998)	Australia, major landform unit of Chan et al. (1986)
10	Holocene alluvium (moderate slopes) (42%) (×6.3), Holocene alluvium (very low slopes) (23%), Pleistocene alluvium (2.1%) (×2.0), others (1.4%)	Cenozoic regolith (38%), sedimentary rocks (38%), granites (10%), metamorphics (6%), others (8%)	Erosional plain (18%), dunefield (14%), plateau (12%), sand plain (10%), rises (10%), low hills (9%), depositional plain (8%)
11	Holocene alluvium (very low slopes) (53%) (×6.6), Pleistocene alluvium (23%) (×2.2), Holocene alluvium (moderate slopes) (18%) (×2.7), others (6%)	Cenozoic regolith (46%), sedimentary rocks (33%), granites (9%), others (12%)	Erosional plain (22%), sand plain (12%), depositional plain (11%), plateau (10%), low hills (9%), dunefield (9%), rises (8%)
12	Holocene alluvium (very low slopes) (72%) (×8.9), Pleistocene alluvium (26%) (×2.5), others (2%)	Cenozoic regolith (72%), sedimentary rocks (17%), others (11%)	Erosional plain (25%), depositional plain (15%), alluvial plain (12%) (×2.8), sand plain (11%), flood plain (8%) (×4.3), plateau (6%), low hills (6%)

Legends with CR of 5% or more are shown. Clusters with SC over ×2.0 are shown in bold text and the factors are in parentheses

^aComposition ratio

^bSpecialization coefficient

^cGeological units were aggregated by lithology and era. The units without an era are rocks older than Mesozoic

platforms. In many regions, Japan and Australia are totally different regarding climate and geological settings. The geological map of Australia (Blake and Kilgour 1998) has over 200 categories, so geologic units were aggregated to 15 categories, considering rock age and lithology. We used all 26 categories of the regolith terrain map of Australia (Chan et al. 1986) as geomorphological data. The regolith terrain map used in this study is at a scale of 1:5,000,000 and valley plains were not represented in sufficient detail. For California, we used the V_{s30} map of Wills et al. (2015), which aggregated and supplemented the geological map of California with estimated seismic amplification.

In a general division between hard rocks and unconsolidated strata, Tables 3 and 5 show that Japan and California are alike in that mountains are formed by bedrocks and plains are formed by sediments. Although there are no Holocene volcanos in California, there are some characteristics in common with Japan; in group 4, volcanic rocks were predominant, and in groups 3 and 5, steep Holocene alluvium that may coincide with talus was predominant. Similar to Japan, groups 6 to 8 were mainly depositional terrains in California. Group 9 was predominant in sandy and gravelly alluvial fans in Japan, but in dry areas of California such as the Basin and Range provinces, it was often distributed in pediplains and bajada that were formed under a dry climate. Although groups 11 and 12 were mainly formed by very low Holocene alluvium like in Japan, Pleistocene alluvium was also distributed and gave some terrain age that was older than that in Japan.

In the case of Australia, groups 1 and 2 were composed of bedrocks, and gentler slopes included more unconsolidated strata like in Japan. However, lithological characteristics for each group were evidently different from Japan and California. All terrain groups in Australia included a similar pair of sedimentary rocks and granites, even in plains. It is well known that bedrocks form erosional plains in Australia after very long-term erosion on the stable continent. This was consistent with our data that erosional plains were predominant in groups 10 to 12, and *SC* values of pediplains were slightly high in groups 10 and 11. Australian mountains showed different predominant lithology in the subcategories a and b, but Cenozoic mafic volcanics appeared in a, though similar lithology often appeared in b in Japan. On the other hand, there were some common points with Japan, that is, alluvial plains, flood plains, and flood outs were predominant in group 12, and lava plains were predominant in groups 4 and 5. It was quite strange that “hills” appeared in all groups in Australia. We thought that there was a possibility that many valley plains were omitted because of the map scale (1:5,000,000; Table 1). Plateaus also appeared in many groups from mountains to plains. In Japan, plateaus

formed by bedrock table mountains as in Australia are rare except for volcanics, and most of the “plateaus” are actually diluvial uplands. In Australia, the difference between plateaus distributed in different groups probably depended on the proportions between tablelands and plateau edges observed in the 280 m grid. Plateaus were especially predominant in group 9, where fan-shape slopes were distributed in Japan and California. The categories with low *CR* (< 5%) that were not described in Table 5 were mainly as follows. Coastal dunes showed high *SC* values in group 5, and glacial features showed the highest *SC* value in group 1b and high *SC* values in groups 3a, 1a, and 2a.

We noted glaciated mountains that were rare in Japan, California, and Australia. Those in the Canadian Rockies and Alps were visually observed using glacier inventory maps (RGI Consortium 2017). The results showed that glacier areas were mainly distributed in groups 1a and 1b, and group 1b covered the areas surrounding glaciers.

Classification map and estimated legends

The final legends for the terrain groups are given in Fig. 12. The descriptions in Fig. 12 were obtained by the methods described in the previous sections. Although this legend mainly shows the groups constructed from Japanese geological and geomorphological information, the main categories that divided the terrain into (1) bedrock mountains; (2) hills; (3) large highland slopes; (4) plateaus, terraces, and large lowland slopes; and (5) plains are probably applicable globally. We noted the landform patterns not only in Japan but also in California and Australia for arid landforms. Figure 13 shows a thumbnail image of global polygon data classified according to the terrain groups in Fig. 12. The classification is obviously improved from Iwahashi and Pike (2007) in representations of terrace shapes (Fig. 14) and landform elements smaller than 1 km (Fig. 15).

Although the global terrain was classified into groups that were categorized using Japanese thematic data, distinct topographies of various locations were also well depicted. For example, terrain classification data from Krasnoyarsk (Fig. 16) clearly depicted lava of Siberian Traps (Svensen et al. 2010). Terrain classification data for central New Zealand (Fig. 17) and the Cameroon line (Fig. 18) also depict well of volcanoes and other mountains in addition to alluvial or coastal lowlands.

In contrast, metropolitan areas, especially in coastal areas, are misclassified as terrace-like groups, i.e., groups 8, 10, and 6 (e.g. Tokyo Gulf Coast in Fig. 14). This is probably caused by DSM (digital surface model) characteristics of the 280 m DEM rather than the influence of artificial slopes. Moreover, limits in the specification of the geometric signatures may still prevent the detection of slight rises in gentle plains. For example, the terrain of the Central

Overview	Terrain group	Landform pattern	Typical landforms in Japan
Bedrock mountain	1a	Steep mountain (rough)	steep mountain of accretionary complex / un-decomposed plutonic rock
	1b	Steep mountain (smooth)	steep mountain of felsic / dissected mafic volcano, escarpment of caldera / fault-block mountain, inselberg
	2a	Moderate mountain (rough)	moderate mountain of felsic volcanic rock / accretionary complex
	2b	Moderate mountain (smooth)	moderate mountain of old sedimentary rock / dissected mafic volcano
Hills	3a	Hills (rough in small and large scale)	hills and mountain footslope of weathered rock
	3b	Hills (smooth in small scale, rough in large scale)	hills of pyroclastic flow deposits / Tertiary sedimentary rock, talus
Large highland slope	4	Upper large slope	un-dissected mafic volcano
	5	Middle large slope	volcanic footslope of debris, dissected escarpment of sediments
Plateau, terrace, large lowland slope	6	Dissected terrace, moderate plateau	hilly terrace, metropolitan areas and coastal industrial areas
	7	Slope in and around terrace or plateau	terrace edge or valley bottom plain in and around terrace
	8	Terrace, smooth plateau	terrace, sand bar, metropolitan areas and coastal industrial areas
	9	Alluvial fan, pediment, bajada, pediplain	alluvial fan, dissected alluvial fan
Plain	10	Alluvial plain, pediplain	alluvial plain in upstream
	11	Alluvial or coastal plain, pediplain	alluvial plain, coastal lowland
	12	Alluvial or coastal plain (gentlest), lake plain, playa	delta, marsh, coastal lowland

Fig. 12 Legend of the terrain classification

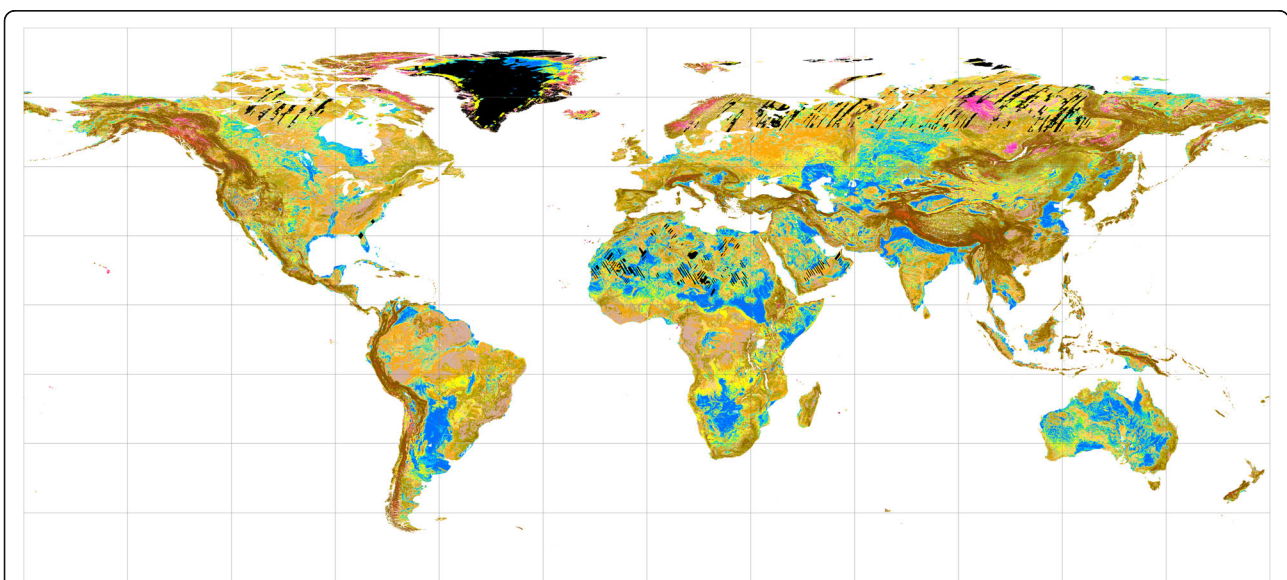
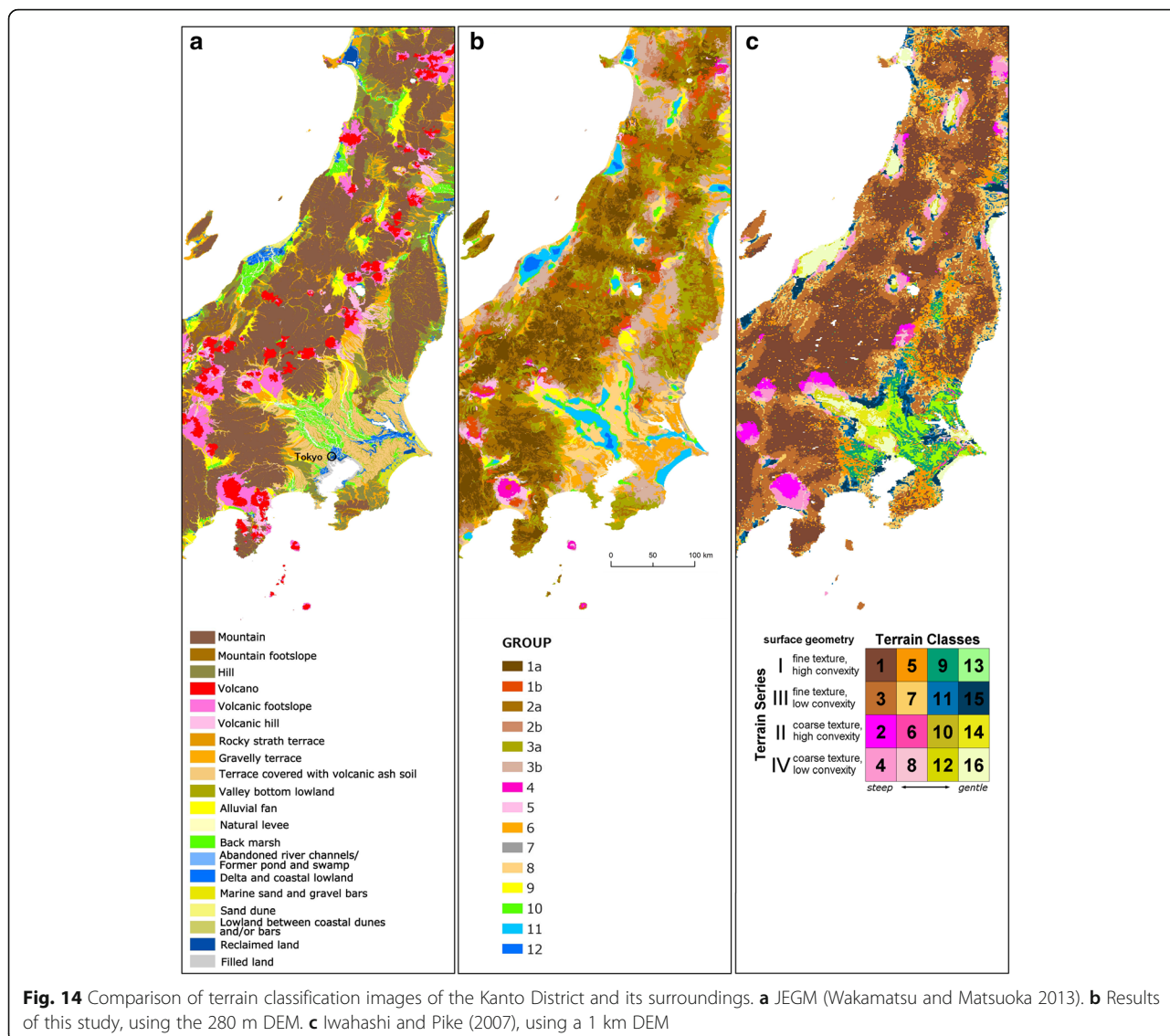


Fig. 13 A thumbnail of global terrain classification. Horizontal and vertical lines coincide with those in Fig. 2. The legend is shown in Fig. 12



Plain of Thailand (Fig. 19) is classified poorly compared with a manual classification map (Ohkura et al. 1989).

Discussion

Validity of the geometric signatures

It is well known that the values and spatial patterns of geometric signatures differ according to the accuracy and resolution of DEMs (Zhang and Montgomery 1994; Armstrong and Martz 2003; Deng et al. 2007; Wu et al. 2007; Maynard and Johnson 2014). Unevenness of DEMs will lead to less accurate classification of topography. For this reason, we used the MERIT DEM for terrain classification.

The three-part geometric signatures adopted in this study generally gave satisfactory results for terrain classification. The new parameter, the combined texture, may help depict both small-scale and large-scale smooth

slopes. In the case of plains, the limit of the description of geometric signatures was mainly caused by insufficient DEM resolution. This problem should be solvable in the future using higher resolution DEMs. For example, the MERIT DEM is originally 3 arc-seconds resolution. However, high-resolution DEMs may create considerable problems in terrain classification owing to the appearance of artificial smoothing or cutting of land. An additional method from using the original elevations, instead of their derivatives, will be needed for more detailed classification of plains because the derivatives may emphasize artificial errors (Erskine et al. 2007).

Tuning of geometric signatures can give very different descriptions, for example, patterns of local convexity changed dramatically with threshold values in calculating convex points (Fig. 7). In this study, we set thresholds of local convexity so as to extract terraces.

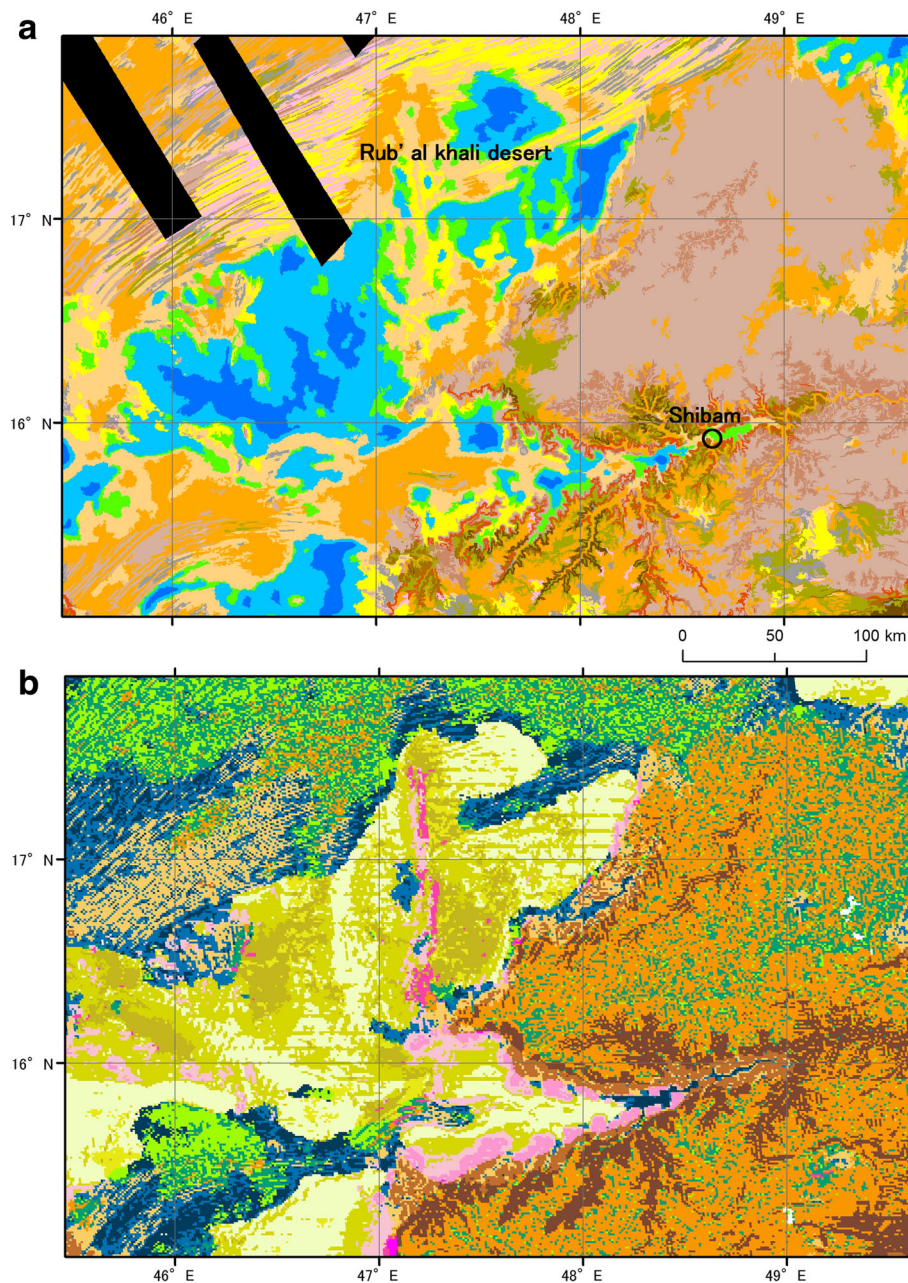


Fig. 15 Comparison of the terrain classification images of the Rub' al khali. **a** Results from of this study, using the 280 m DEM. **b** Iwahashi and Pike (2007), using a 1 km DEM

However, different threshold values might possibly output better classification results for other purposes or other DEMs.

Considering the calculation cost and expected degree of improvement, and the ability to add another parameter later because the threshold processing had been performed using combined texture, we did not think that the addition of another geometric signature was necessary for clustering. However, the mixture of depositional landforms and erosional landforms (e.g., fans and

pediplains in group 9) seems to be a major problem in continental regions where both alluvial landforms and arid landforms exist.

Validity of the region segmentation and clustering

In terms of region segmentation, we did not think that many parameters were necessary for drawing boundary lines of landforms, and the results of object segmentation using LN slope and local convexity effectively separated the range of similar landform

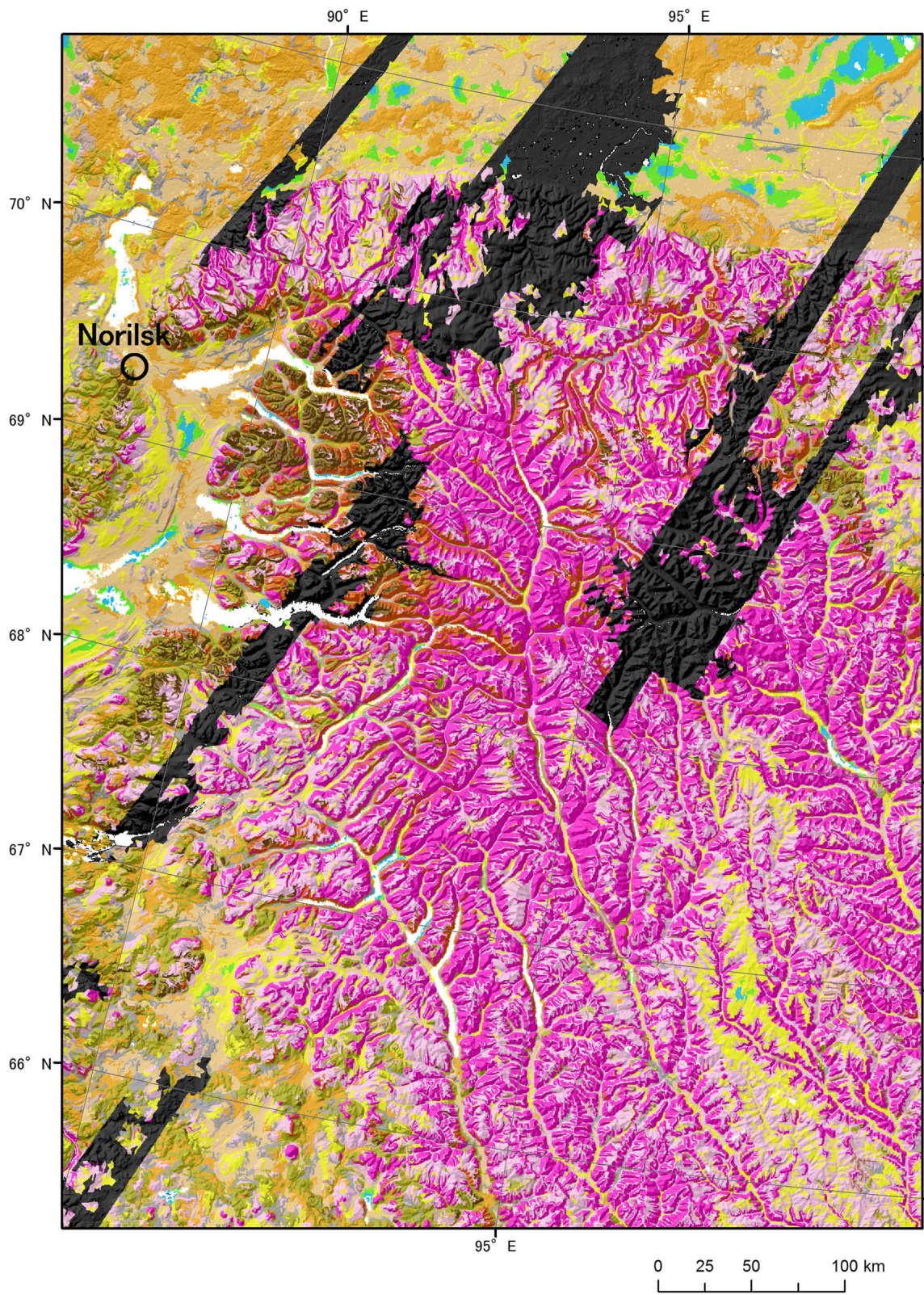


Fig. 16 Shaded terrain classification image in the Krasnoyarsk region (Russia)

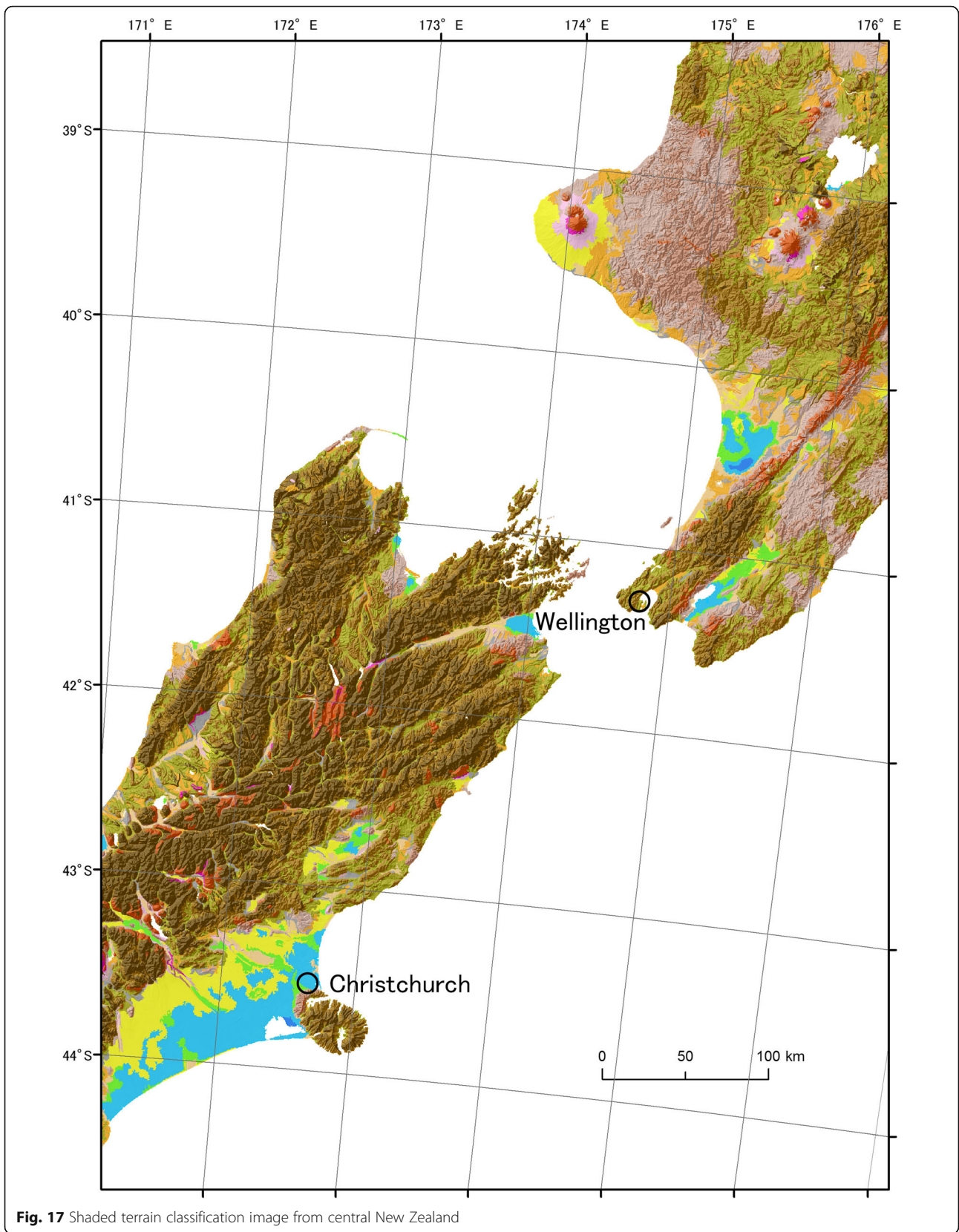
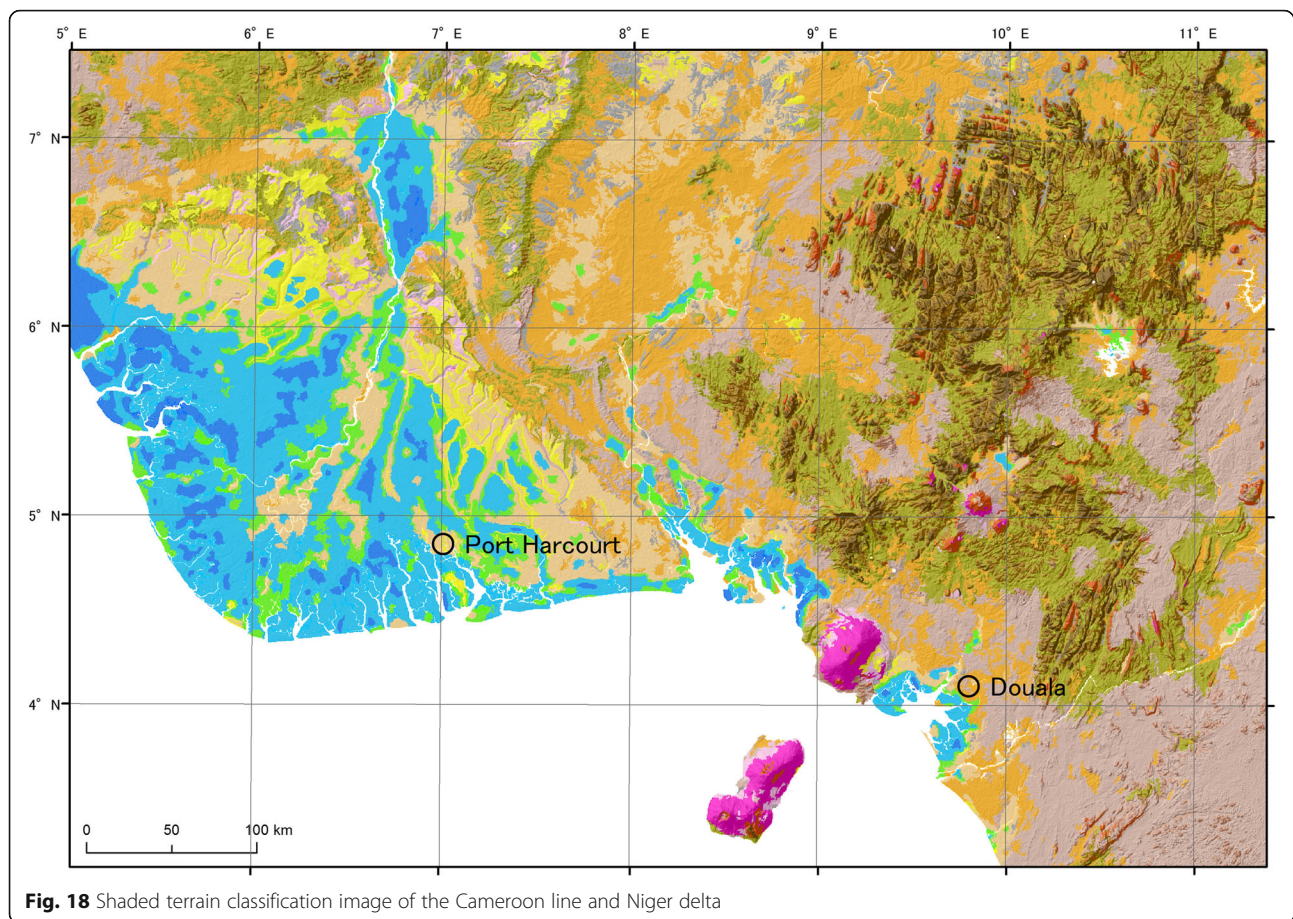


Fig. 17 Shaded terrain classification image from central New Zealand



patterns as considered in the section “Region segmentation”. A scale parameter of 20 seems to be rather small on continents, but is mostly adequate (or rather too large) for Japan where various micro geomorphological elements are distributed. Smaller values for the scale parameter will create a large volume of polygon data and will make it difficult to use the data. We thought 20 was adequate globally for the scale parameter. The polygon-based format helps to edit or merge terrain classification data easily.

The 40 clusters obtained by *k*-means clustering were globally common divisions, because the clustering was done using all polygon attributes. Although the final number of clusters is arbitrary in *k*-means clustering, the calculation cost tends to increase as the number of clusters increases, and the calculation does not converge with too many clusters. Moreover, too many clusters will make data usage rather difficult. Considering this, we decided on the final number of clusters as 40.

Validity of the grouping and reclassification

In the hierarchical clustering in Japan, bedrock mountains constituted clearly separate branches from other

terrain types. The difference of geological and geomorphological characteristics between bedrock mountains and others was relatively clear. Among the bedrock mountains and hills, we distinguished two types of slopes, sub-categories a and b. Suzuki (2002) gives a schematic diagram showing the relationship between the relief and drainage density, and the strength and permeability of bedrock. The diagram shows that hard rocks form high-relief mountains, soft rocks form low-relief mountains (or hills), low permeability rocks form straight slopes, and high permeability rocks form convex slopes. Surface texture (i.e., the density of pits and peaks that coincide with valley lines and ridges in the 280 m grid scale) is related to drainage density, and local convexity is related to the convexity of slopes. In sub-category b, which had a lower drainage density than a, highly permeable types of rocks such as old mafic volcanic rocks and sedimentary rocks were more predominant than very hard rocks such as accretionary complex and metamorphic rocks. This was consistent with the findings of Suzuki (2002) and indicated that it may be permeability that separates a and b of mountains and hills in Japan. Indeed, groups 1b and 2b were predominant in crushed or high permeability rocks such as

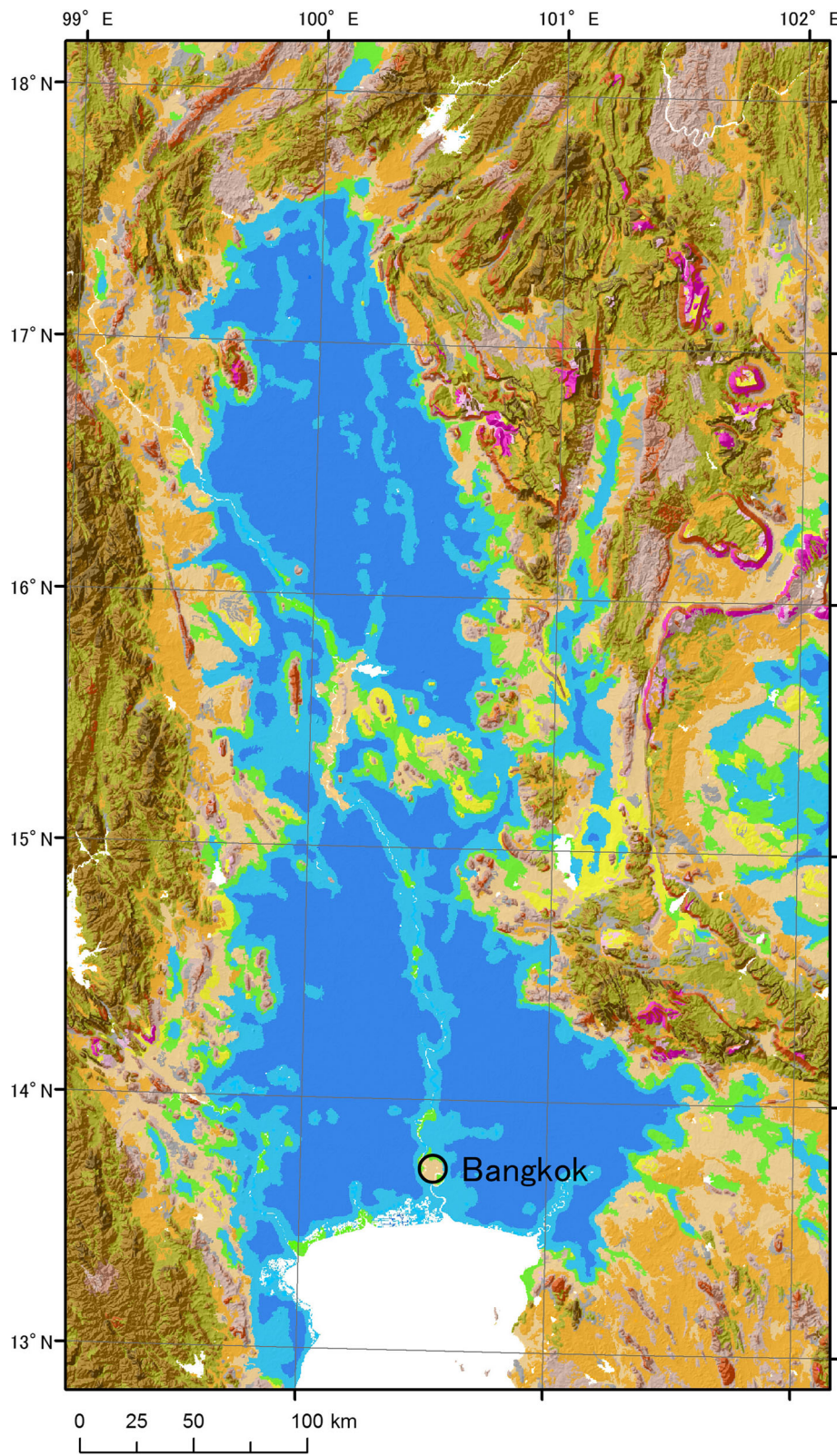


Fig. 19 Shaded terrain classification image of the Central Plain of Thailand and its surroundings

weathered lava and old sedimentary rocks in Japan and showed lower V_{s30} values (Fig. 11). Groups 4 and 5 were unique groups; they were clearly predominant in undissected mafic volcanos and volcanic footslopes in Japan and showed very high correlation with the sediment disaster hazard area (Table 4). Not exactly the same, but similar lithologic trends of groups 4 and 5 could be observed even in California and Australia. The relationship between lithology and landforms in mountains has been explored in various ways, e.g., the relationship between slope materials and slope surface (Kenter 1990) and rock control (Yatsu 1966). Moreover, lithology and rock hardness have broad study fields in engineering geology and have been widely discussed for rock mass classification since Terzaghi (1946). Some rock mass classifications focus on classification of lithology (e.g., Marinos and Hoek 2000). Thus, especially under the same climatic and geologic province, searching for similar topography in mountains and hills may help to at least grasp some common points of physical properties of the ground.

Intermediate landforms formed by half- or unconsolidated strata were relatively difficult to classify. They converged to the “alluvial or coastal plains and non-volcanic terraces” branch and a “volcanos, hills, fans, terraces” branch in Japan (Fig. 9). Among them, groups 7 and 9 were included in the “volcanos, hills, fans, terraces” branch-like large highland slopes (groups 4 and 5) in spite of their gentler inclinations. Groups 7 and 9 sometimes appeared in volcanic footslopes and indicated that they were depositional slopes of debris.

In the case of plains in Japan, the clusters included in groups 8, 10, 11, and 12, which had a high ratio of historical liquefaction, were all categorized into the “alluvial or coastal plains and non-volcanic terraces” branch. Group 6, which partly included the clusters categorized into the branch, showed a slightly high ratio of historical liquefactions. In total, the result of grouping using Japanese geomorphological and geological data is generally suitable for distinguishing lowlands, terraces, debris slopes, hills, bedrock mountains, and large slopes, especially those formed by Holocene mafic volcanos. However, as suggested by the comparison with liquefaction data, the limit of the description of geometric signatures appears in failures to detect narrow valley bottom plains. Slightly high terrains in gentle plains may also be missed. Moreover, DSM characteristics of the 280 m DEM and artificial slopes gave less accurate classification in metropolitan areas.

Regional differences and future scope

In this study, we grouped clusters and determined the legend using Japanese geological and geomorphological

information. The Japanese Islands lie on monsoonal mountainous regions in a young orogenic belt, and Japanese mountains are mainly formed by accretionary wedges and volcanic rocks younger than the Jurassic. Oguchi et al. (2001) characterized Japanese landforms by steep watersheds, heavy storms, frequent slope failures and landslides, large flood discharge and efficient sediment transport, high sediment yields, and catastrophic hydro-geomorphological events associated with earthquakes and volcanic eruption plains. There are very few or no distributions of erosional plains, glacial landforms, and Eolian landforms in Japan. In geomorphological maps, the necessary legend may vary from region to region. For example, Oya (1995) compared the legends of European and Japanese geomorphological maps and pointed out that in Europe, the classification focused on climatic geomorphology and erosional geomorphology, but that in Japan, on depositional geomorphology and less on glacial geomorphology and karst geomorphology. In recognition of this difference, it is important to determine whether the grouping based on Japan can be dealt with by simply replacing the legend in other areas, or if it is fundamentally insufficient. In addition, it is important to know whether both the topography and surface material are similar, even if the landform process is different (e.g., Japanese alluvial fans and pediplains in arid regions), or if the surface material is also different.

As mentioned earlier, mountains in Japan, California, and Australia are mainly composed of bedrocks, and in Japan and California, plains are commonly composed of unconsolidated strata. However, observing intermediate and gentle slopes globally, we noticed a problem that depositional fans formed by unconsolidated strata and erosional plateaus/pediplains formed by old rocks were grouped into the same groups, especially into group 9. These phenomena were observed not only in Australia but also in other shield and platform regions such as the Northeast China Plain, the Interior Plains of North America, and the European Plain. We thought that information from the global geologic province was necessary to perform better terrain classification that responds to regional needs. Nonetheless, although small-scale data exist (e.g., USGS <https://earthquake.usgs.gov/data/crust/type.html>), we did not have global geologic province data that matched the 280 m grid scale. We thought that it is possible to solve this by replacing the legend because of the advantages of polygon data; however, attention is needed for mixed areas where both depositional and erosional gentle plains exist. These clear differences of lithological conditions in gentler landforms may be an important further research task, because markedly different lithology with similar topography indicates a marked difference of landform processes.

Conclusions

This study used the MERIT DEM produced by Yamazaki et al. (2017) who removed multiple error components from existing space-borne DEMs. As a result, it was possible to perform terrain classification that excluded the influence of DEM errors as much as possible. Multi-resolution segmentation was performed to classify homogeneous geomorphological elements. Terraces, plateaus, and fans, which were likely to be missed on a coarse DEM but important for human habitats, were effectively extracted from plains by segmentation using LN slope and local convexity. Terrain classification was performed by adding surface texture data to LN slope and local convexity. We adopted a machine learning method, *k*-means clustering, for terrain classification. The 40 clusters obtained by *k*-means clustering were prepared for globally common divisions. We grouped clusters of similar properties by hierarchical clustering using Japanese thematic maps, and after that, we reclassified mountains and hills using combined texture. The final 15 groups were cross tabulated and again visually compared with Japanese thematic maps to construct a legend. We tried to attach geomorphological meanings to the classification results according to the cross tabulations with geological or geomorphological maps. We also conducted the same analysis using data for California and Australia to check the legend. The legend mainly showed terrain groups based on Japanese geological and geomorphological information; however, the main categories that separated the terrain into (1) bedrock mountains, (2) hills, (3) large highland slopes, (4) plateaus, terraces, large lowland slopes, and (5) plains were probably applicable globally. Distinct topographies in various specific areas were also well depicted. In general, the terrain classification was obviously improved from Iwahashi and Pike (2007) in the representation of terrace shape and landform elements smaller than 1 km. However, narrow plains at the foot of mountains, metropolitan areas, and slight rises in gentle plains were not classified sufficiently because of the limit of the description of geometric signatures. These problems may be caused by insufficient resolution and the DSM characteristics of the 280 m DEM. In addition, there may be room for improvement in tuning the geometric signatures. Observing intermediate and gentle slopes globally, we noticed that depositional fans formed by unconsolidated strata and erosional plateaus/pediains formed by old rocks were grouped into the same groups. Although we thought that it was possible to deal with this by replacing the legend because of the advantage of polygon data, attention was necessary for mixed areas where both depositional and erosional gentle plains existed.

Further studies are needed to complete global terrain classification, perhaps using the original 3 arc-second MERIT DEM, with better tuning of the geometric

signatures. Moreover, the groupings of the clusters need more variation in response to locality. Successful classification of geomorphological terrain types may lead to better understanding of terrain susceptibility to natural hazards, which is especially vital in populated areas, and will help land development in areas where geological information does not exist.

Additional file

Additional file 1: Cross tabulation results and graphs with the reference numbers of clusters in Japan. (PDF 530 kb)

Abbreviations

CR: Composition ratio; CSC: Corrected specialization coefficient; DEM: Digital elevation model; DID: Densely inhabited districts; GIS: Geographic information system; JEGM: Japan Engineering Geomorphologic Classification Map; LN slope: Logarithmic converted slope gradient; MERIT DEM: Multi-error-removed improved-terrain DEM; SC: Specialization coefficient; SDGM: Seamless Digital Geological Map of Japan; Vs30: Average shear wave velocity for the top 30 m

Acknowledgements

We are deeply grateful to Richard J. Pike who helped the corresponding author with expanding the numerical terrain classification work from a domestic to a global scale, Sayuri Mochiki who helped data generation of terrain classification, and Alan Yong of the U. S. Geological Survey and Patcharavadee Thamarux of the Tokyo Institute of Technology who discussed the terrain classification with us. We thank Jun Matsumoto of Tokyo Metropolitan University and the anonymous referees for their most helpful reviews.

Funding

This work is supported by JSPS KAKENHI Grant Number 15K01176.

Authors' contributions

JI designed the study, analyzed the data, and drafted the manuscript. IK helped in the design of digital filtering using DEM. MM prepared the Vs30 material. DY prepared the DEM. All authors read and approved the final manuscript.

Competing interests

The authors declare that they have no competing interest.

Publisher's Note

Springer Nature remains neutral with regard to jurisdictional claims in published maps and institutional affiliations.

Author details

¹Geospatial Information Authority of Japan, Geography and Crustal Dynamics Research Center, Kitasato 1, Tsukuba, Ibaraki 305-0811, Japan. ²Japan Digital Road Map Association, Hirakawa 1-3-13, Chiyoda-ku, Tokyo 102-0093, Japan. ³Interdisciplinary Graduate School of Science and Technology, Tokyo Institute of Technology, Nagatsuta 4259-G3-2, Midori-ku Yokohama, Kanagawa 226-8502, Japan. ⁴Institute of Industrial Science, The University of Tokyo, Tokyo, Japan.

Received: 31 March 2017 Accepted: 7 December 2017

Published online: 05 January 2018

References

- Ariza-Villaverde AB, Jiménez-Hornero FJ, Gutiérrez de Ravé E (2015) Influence of DEM resolution on drainage network extraction: a multifractal analysis. *Geomorphology* 241:243–254
- Armstrong RN, Martz LW (2003) Topographic parameterization in continental hydrology: a study in scale. *Hydrol Process* 17:3763–3781

- Baatz M, Schäpe A (2000) Multiresolution segmentation: an optimization approach for high quality multi-scale image segmentation. In: Strobl J, Blaschke T, Greisner G (eds) *Angewandte Geographische Informations-Verarbeitung XII*. Wichmann Verlag, Karlsruhe
- Blake DH, Kilgour B (1998) Geological Regions of Australia 1:5 000 000 scale, Geoscience Australia. <http://www.ga.gov.au/metadata-gateway/metadata/record/32366>. Accessed 15 Oct 2017
- Bontemps S, Defourny P, Radoux J, Van Bogaert E, Lamarche C, Achard F, Mayaux P, Boettcher M, Brockmann C, Kirches G, Zülke M, Kalogirou V, Arino O (2013) Consistent Global Land Cover Maps for Climate Modeling Communities: Current Achievements of the ESA's Land Cover CCI. ESA Living Planet Symposium 9–13 September 2013, Edinburgh, United Kingdom
- Chan RA, Craig MA, D'Addario GW, Gibson DL, Ollier CD, Taylor G (1986) The regolith terrain map of Australia 1:5,000,000. Bureau of Mineral Resources, Geology and Geophysics Record 1986/27
- Danielson JJ, Gesch DB (2011) Global Multi-resolution Terrain Elevation Data 2010 (GMTED2010). U. S. Geological Survey Open-File Report 2011–1073
- De Reu J, Bourgeois J, Bats M, Zwertvaegher A, Gelorini V, Smedt PD, Wei C, Antrop M, De Maeyer P, Finke P, Van Meirvenne M, Vermiers J, Crombe P (2013) Application of the topographic position index to heterogeneous landscape. *Geomorphology* 186:39–49
- del Val M, Iriarte E, Arriolabengoa M, Aranburu A (2015) An automated method to extract fluvial terraces from LIDAR based high resolution digital elevation models: the Oiartzun valley, a case study in the Cantabrian Margin. *Quat Int* 364:35–43
- Deng Y, Wilson JP, Bauer BO (2007) DEM resolution dependencies of terrain attributes across a landscape. *Int J Geogr Inf Sci* 21:187–213
- Dikau R, Brabb EE, Mark RM (1991) Landform classification of New Mexico by computer. U. S. Geological Survey Open-File Report 91–634
- Drăguț L, Blaschke T (2006) Automated classification of landform elements using object-based image analysis. *Geomorphology* 81:330–344
- Drăguț L, Eisank C (2012) Automated object-based classification of topography from SRTM data. *Geomorphology* 141–142:21–33
- Erskine RH, Green TR, Ramirez JA, MacDonald LH (2007) Digital elevation accuracy and grid cell size: effects on estimated terrain attributes. *Soil Sci Soc Am J* 71:1371–1380
- Evans IS (1980) An integrated system of terrain analysis and slope mapping. *Zeitschrift für Geomorphologie, Supplement Band* 36:274–295
- Gallant J (2011) Adaptive smoothing for noisy DEMs. *Proc Geomorphometry* 33:7–9
- Geological Survey of Japan, AIST (ed.) (2015) Seamless digital geological map of Japan 1: 200,000. May 29, 2015 version. Geological Survey of Japan, National Institute of Advanced Industrial Science and Technology
- Guida D, Cuomo A, Palmieri V (2016) Using object-based geomorphometry for hydro-geomorphological analysis in a Mediterranean research catchment. *Hydro Earth Syst Sci* 20:3493–3509
- Guth PL (2006) Geomorphometry from SRTM: comparison to NED. *Photogramm Eng Remote Sens* 72:269–277
- Hartmann J, Moosdorf N (2012) The new global lithological map database GLIM: a representation of rock properties at the Earth surface. *Geochemistry, Geophysics, Geosystems* 13. <https://doi.org/10.1029/2012GC004370>
- Hengl T, Mendes de Jesus J, Heuvelink GBM, Ruiperez Gonzalez M, Kilibarda M, Blagotić A, Wei S, Wright MN, Xiaojuan G, Bauer-Marschallinger B, Guevara MA, Vargas R, MacMillan RA, Batjes NH, Leenaars JGB, Ribeiro E, Wheeler I, Mantel S, Kempen B (2017) SoilGrids250m: global gridded soil information based on machine learning. *PLoS One* 12:e0169748. <https://doi.org/10.1371/journal.pone.0169748>
- Hough SE, Altidor JR, Anglade D, Given D, Janvier MG, Maharrey JZ, Mark Meremonte M, Mildor BS, Prepetit C, Yong A (2010) Localized damage caused by topographic amplification during the 2010 M 7.0 Haiti earthquake. *Nat Geosci* 3:778–782
- Iwahashi J (1994) Development of landform classification using the digital elevation model. *Dis Prev Res Inst Annuals* 37B:141–156 (in Japanese with English abstract and figures)
- Iwahashi J, Kamiya I (1995) Landform classification using digital elevation model by the skills of image processing—mainly using the Digital National Land Information. *Geoinformatics* 6:97–108 (in Japanese with English abstract)
- Iwahashi J, Kamiya I, Matsuoka M (2010) Regression analysis of Vs30 using topographic attributes from a 50-m DEM. *Geomorphology* 117:202–205
- Iwahashi J, Matsushi Y, Fukuoaka H (2015) Digital terrain analysis of sea-land combined data on the outer zone of Southwest Japan including the Nankai Trough. *Disaster Prev Res Inst Annuals* 58B:102–115
- Iwahashi J, Pike RJ (2007) Automated classification of topography from DEMs by an unsupervised nested-means algorithm and a three-part geometric signature. *Geomorphology* 86:409–440
- Japan Society of Civil Engineering (2016) Standard specifications for Tunneling—2016, mountain tunnels. Maruzen Publishing Co. Ltd, Tokyo (in Japanese)
- Jasiewicz J, Netzel P, Stepinski TF (2014) Landscape similarity, retrieval, and machine mapping of physiographic units. *Geomorphology* 221:104–112
- Jennings CW (1977) Geologic map of California. California Division of Mines and Geology
- Kavzoglu T, Yildiz M (2014) Parameter-based performance analysis of object-based image analysis using aerial and Quikbird-2 images. *ISPRS Annals Photogrammetry Remote Sens Spatial Inform Sci* II-7:31–37
- Kenter JAM (1990) Carbonate platform flanks: slope angle and sediment fabric. *Sedimentology* 37:777–794
- MacMillan RA, Martin TC, Earle TJ, McNabb DH (2003) Automated analysis and classification of landforms using high-resolution digital elevation data: applications and issues. *Can J Remote Sens* 29:592–606
- MacQueen JB (1967) Some methods for classification and analysis of multivariate observations. In: *Proceedings of 5-th Berkeley symposium on mathematical statistics and probability*, vol 1. University of California Press, Berkeley, pp 281–297
- Marinos P, Hoek E (2000) GSI: a geologically friendly tool for rock mass strength estimation. In: *Proceedings of GeoEng2000 conference*, Melbourne. Technomic Publishing, Pennsylvania
- Martha TR, Kerle N, Jetten V, van Westen CJ, Kumar KV (2010) Characterizing spectral, spatial and morphometric properties of landslides for semi-automatic detection using object-oriented methods. *Geomorphology* 116:24–36
- Maynard JJ, Johnson MJ (2014) Scale-dependency of LiDAR derived terrain attributes in quantitative soil-landscape modeling: effects of grid resolution vs. neighborhood extent. *Geoderma* 230–231:29–40
- Meybeck M, Green P, Vörösmarty C (2001) A new typology for mountains and other relief cases: an application to global continental water resources and population distribution. *Mt Res Dev* 21:34–45
- Nelson A, Reuter HI, Gessler P (2009) DEM production methods and sources. In: Hengl T, Reuter HI (eds) *Geomorphometry concepts, software, applications*. Elsevier, Amsterdam
- Oguchi T, Saito K, Kadomura H, Grossman M (2001) Fluvial geomorphology and paleohydrology in Japan. *Geomorphology* 39:3–19
- Ohkura H, Haruyama S, Oya M, Vibulsresth S, Simking R, Suwanwerakamton R (1989) A geomorphological land classification for the flood-inundated area in the Central Plain of Thailand using satellite remote sensing technology. *Res Notes Nat Res Center Disaster Prev* 83:25 (in Japanese with English abstract; 1 map sheet in English)
- Otofuji Y, Matsuda T, Nohda S (1985) Opening mode of the Japan Sea inferred from the palaeomagnetism of the Japan Arc. *Nature* 317:603–604
- Oya M (1995) Geomorphological maps of alluvial plains and their utilization for mitigation of natural hazards: flooding and soil liquefaction. *Geogr Rev Japan* 68B:218–242
- Pike RJ (1988) The geometric signature: quantifying landslide-terrain types from digital elevation models. *Math Geol* 20:491–511
- RGI Consortium (2017) Randolph Glacier Inventory – A Dataset of Global Glacier Outlines: Version 6.0. Technical Report, Global Land Ice Measurements from Space, Colorado, USA. Digital Media. <https://doi.org/10.7265/N5-RGI-60>
- Sayre R, Dangermond J, Frye C, Vaughan R, Aniello P, Breyer S, Cribb D, Hopkins D, Nauman R, Derrenbacher W, Wright D, Brown C, Convis C, Smith J, Benson L, VanSistine DP, Warner H, Cress J, Danielson J, Hamann S, Cecere T, Reddy A, Burton D, Grosse A, True D, Metzger MJ, Hartmann J, Moosdorf N, Dürr HH, Paganini M et al (2014) A new map of global ecological land units—an ecophysiological stratification approach. Association of American Geographers, Washington, DC https://rmgsc.cr.usgs.gov/ecosystems/docs/AAG_Global_Ecosystems_Booklet.pdf
- Shafique M, van der Meijde M, van der Werff HMA (2012) Evaluation of remote sensing-based seismic site characterization using earthquake damage data. *Terra Nova* 24:123–129
- Speight JG (1984) Landform. In: *Australian soil and land survey field handbook*, First edn. Inkata Press, Melbourne
- Suzuki T (2002) Rock control in geomorphological processes: research history in Japan and perspective. *Trans Jpn Geomorphol* 23:161–199
- Svensen H, Planke S, Polozov AG, Schmidbauer N, Corfu F, Podladchikov YY, Jamtveit B (2010) Siberian gas venting and the end-Permian environmental crisis. *Earth Planet Sci Lett* 277:490–500

- Terzaghi K (1946) Rock defects and loads on tunnel supports. Rock tunneling with steel supports, In
- van Asselen S, Seijmonsbergen AC (2006) Expert-driven semi-automated geomorphological mapping for a mountainous area using a laser DTM. *Geomorphology* 78:309–320
- Wakamatsu K (2011) Maps for historic liquefaction sites in Japan, 745–2008. University of Tokyo Press, Tokyo
- Wakamatsu K, Matsuoka M (2013) Nationwide 7.5-arc-second Japan engineering geomorphologic classification map and Vs30 zoning. *J Disaster Res* 8:904–911
- Wills CJ, Gutierrez CI, Perez FG, Branum DM (2015) A next generation Vs30 map for California based on geology and topography. *Bull Seismol Soc Am* 105:3083–3091
- Wills CJ, Petersen M, Bryant WA, Reichele M, Saucedo GJ, Tan S, Taylor G, Treiman J (2000) A site-conditions map for California based on geology and shear-wave velocity. *Bull Seismol Soc Am* 90:S187–S208
- Wu S, Li J, Huang GH (2007) Modeling of the effects of elevation data resolution on the performance of topography-based watershed runoff simulation. *Environ Model Softw* 22:1250–1260
- Yamazaki D, Ikeshima D, Tawatari R, Yamaguchi T, O'Loughlin F, Neal JC, Sampson CC, Kanae S, Bates PD (2017) A high-accuracy map of global terrain elevations. *Geophys Res Lett* 44:5844–5853
- Yatsu E (1966) Rock control in geomorphology. Sozosha, Tokyo
- Yong A, Hough SE, Iwahashi J, Braverman A (2012) A terrain-based site-condition map of California with implications for the contiguous United States. *Bull Seismol Soc Am* 102:114–128
- Zevenbergen LW, Thorne CR (1987) Quantitative analysis of land surface topography. *Earth Surf Process Landf* 12:47–56
- Zhang W, Montgomery DR (1994) Digital elevation model grid size, landscape representation, and hydrologic simulations. *Water Resour Res* 30:1019–1028

Submit your manuscript to a SpringerOpen[®] journal and benefit from:

- ▶ Convenient online submission
- ▶ Rigorous peer review
- ▶ Open access: articles freely available online
- ▶ High visibility within the field
- ▶ Retaining the copyright to your article

Submit your next manuscript at ▶ springeropen.com
